Analysis of Geomagnetic Disturbance (GMD) Related Harmonics

3002002985

Analysis of Geomagnetic Disturbance (GMD) Related Harmonics

3002002985

Technical Update, March 2014

EPRI Project Manager

J. Taylor

ELECTRIC POWER RESEARCH INSTITUTE
3420 Hillview Avenue, Palo Alto, California 94304-1338 ▪ PO Box 10412, Palo Alto, California 94303-0813 ▪ USA 800.313.3774
650.855.2121 ▪ askepri@epri.com ▪ www.epri.com

DISCLAIMER OF WARRANTIES AND LIMITATION OF LIABILITIES

THE FOLLOWING ORGANIZATION, UNDER CONTRACT TO EPRI, PREPARED THIS REPORT:

Walling Energy Systems Consulting, LLC

This is an EPRI Technical Update report. A Technical Update report is intended as an informal report of continuing research, a meeting, or a topical study. It is not a final EPRI technical report.

NOTE

For further information about EPRI, call the EPRI Customer Assistance Center at 800.313.3774 or e-mail askepri@epri.com.

ACKNOWLEDGMENTS

The following organization, under contract to the Electric Power Research Institute (EPRI), prepared this report:

Walling Energy Systems Consulting, LLC
438 Vischer Ferry Road
Clifton Park, NY 12065-1622

Principal Investigator
R. Walling

This report describes research sponsored by EPRI.

This publication is a corporate document that should be cited in the literature in the following manner:

Analysis of Geomagnetic Disturbance (GMD) Related Harmonics. EPRI, Palo Alto, CA: 2014. 3002002985.

ABSTRACT

This report describes an investigation of the characteristics of harmonic distortion caused by transformers during a geomagnetic disturbance (GMD) and a scoping assessment of tools needed by the industry to perform an adequate assessment of GMD-related distortion impacts. Because single-phase transformers are typically the most critical and most significant—as well as the most straightforward to model and explain—the asymmetric saturation behavior of these transformers is the scope of this report. When the results of a properly performed harmonic assessment are combined with the fundamental frequency analyses, a much more accurate evaluation of grid security during GMDs can be obtained.

This report provides technical background and a tutorial discussion on the basics of asymmetric saturation. Harmonic current generation by geomagnetic-induced-current- (GIC-) saturated transformers is characterized, as well as the relationships of these currents to significant parameters such as GIC magnitude and transformer characteristics. Injection of transformer exciting current into the grid results in voltage distortion, and this distortion affects the generation of harmonics. The non-ideal nature of the source characteristics of harmonic currents created by GIC-saturated transformers is extensively explored.

Keywords
Geomagnetic disturbance (GMD)
Geomagnetic-induced current (GIC)
Geomagnetic storm scenario
Harmonics
Solar storm
Space weather

CONTENTS

LIST OF FIGURES

LIST OF TABLES

1 INTRODUCTION

Overview

Solar disturbances, such as coronal mass ejections, can result in a terrestrial geomagnetic disturbance (GMD) when charged particles emitted from the sun interact with the earth's magnetic field. GMDs can result in the flow of very low frequency geomagnetically-induced currents (GIC) in power systems. The physics of this phenomenon have been extensively documented in the literature [1]. Basically, the transmission lines and the return path through the earth, closed through grounded-wye transformers, form a loop enclosing the slowly-changing magnetic field produced by auroral electrojet currents flowing in the upper atmosphere. Because the spectral content of the GIC induced in this loop is composed of very low frequencies, it can be considered essentially dc (i.e., quasi-dc) for most practical purposes.

The voltage induced in the transmission line-earth loop integrates to impose a quasi-dc flux bias on the transformers closing the loop. This includes both grounded-wye transformers closing the connection between the transmission system and earth, as well as the series windings of autotransformers providing a dc path between different transmission voltage levels. The flux bias results in asymmetric, or part-cycle, saturation of the transformers, producing unusually large and highly-distorted exciting currents. The exciting currents drawn by the asymmetrically-saturated transformers are composed of both even- and odd-order harmonic components, a fundamental current component, and a dc component that is equal to the GIC flow. While the asymmetric saturation is commonly viewed as being "caused" by the GIC, it is actually the quasi-dc voltage induced in the loop that causes the saturation, and after saturation occurs the GIC can rise to the steady state value equal to the driving quasi-dc voltage divided by the loop resistance.

Asymmetric saturation of a transformer can have direct impact on the transformer itself, and may also have profound impacts on the power system performance via the large exciting currents drawn from the transmission system, regardless of whether the saturation poses any risk to the transformer. The potential for direct impacts of GIC saturation on transformers is widely recognized and is presently the subject of much controversy. Some have speculated that a severe but credible GMD event could result in the wide-scale failure of numerous critical power transformers [2]. Others, including many transformer experts, see the risk as limited to particular and generally-limited number of transformer designs, and assert that widespread transformer damage is unlikely [3].

The fundamental (e.g., 60 Hz) exciting current component of a saturated transformer is in phase with the fundamental frequency flux of the transformer, which lags the applied fundamental voltage by ninety degrees. Thus, this fundamental component is reactive current; i.e., the saturated transformer absorbs reactive power. With many transformers in a transmission system asymmetrically saturated at the same time during a major GMD event, the transformers in aggregate impose a potentially large reactive power demand on the grid. There is general consensus that the cumulative reactive power demand of many affected transformers in a very severe GMD could result in grid collapse via voltage or angular instability [4].

Recognized, but perhaps underappreciated, is the role that harmonic currents and voltages can play during a GMD, potentially aggravating the power system performance impacts caused by fundamental-frequency reactive demand. Asymmetrically-saturated transformers are potential sources of high-magnitude harmonic currents at harmonic orders (i.e., even order harmonics) not normally seen at any significant magnitude in the power system on other than a transient basis, such as the inrush phenomenon immediately following transformer energization. Because severe GMDs are wide-scale events, numerous transformers throughout a transmission system will be saturated simultaneously. Thus, during a severe GMD, the transmission system will have many sources of harmonic current injecting in synchronism, with defined phase relationships to the fundamental voltage at each transformer location. As a result, the various injections create harmonic current and voltage components at a particular location that may superimpose destructively, such as to cancel each other, or constructively such as to increase the magnitudes of harmonic voltage and current components. The injected harmonics also may interact with system resonances that have the potential to greatly amplify, or attenuate, harmonic voltages and currents.

Ordinary power quality criteria are not the critical concern during severe GMD. Potentially extreme values of harmonic voltage and current distortion, however, can impose substantial physical stresses on power system components and may cause misoperation of protection and control systems. The most vulnerable power equipment includes capacitor banks and synchronous generators. High harmonic current levels can either damage this equipment or force their protective tripping. Capacitor banks and generators supply the majority of a system's reactive power resources, and their tripping or failure remove reactive sources at a time when the grid is subjected to the significantly increased reactive power demands of the GIC-saturated transformers. In addition to physically vulnerable equipment, control and protection systems are vulnerable to incorrect operation, potentially removing critical system components during the midst of a GMD. The harmonics injected into the system during GMD may, as a consequence of the physical and protection impacts resulting in critical line or equipment tripping, can potentially aggravate fundamental-frequency voltage stability issues. Thus, the critical concern regarding harmonics during GMD is not their impact on power quality in the conventional sense, but rather the potential impact of the harmonics on grid security.

Assessments of bulk system operational security using only fundamental frequency analysis (e.g., load flow and dynamic stability) may underestimate the risks of severe GMD. A more complete assessment should consider the harmonic effects; particularly where they cause loss of reactive support, increase reactive demand, and increase the probability of faults and other abrupt disturbances that could trigger system instability and collapse. System harmonic performance evaluation for GMD events, however, is particularly challenging due to the following factors:

- GMD results in a large number of coherent harmonic sources distributed throughout the transmission grid (coherent meaning that the phase relationships between the various harmonic sources are deterministic, rather than stochastic). Many harmonic analysis tools are not configured to accommodate numerous sources.
- Current injections are over a range of harmonic frequencies, including both even and odd orders.

- Harmonic voltage distortion interacts with the transformers to alter the magnitude and phase of the injected harmonic currents; i.e., saturated transformers do not behave as ideal harmonic current sources.
- The harmonic source characteristics of three-phase transformers are complex, and the sequence components of the harmonics produced do not appear exclusively in the classic pattern (e.g., positive and negative sequence components of three-phase transformer exciting currents include triplen harmonics, and non-triplen harmonics have zero-sequence components).
- Propagation of the harmonics produced by GIC saturation is in both the ground mode (zero sequence) as well as the line modes (positive and negative sequence). Many harmonic analysis tools are not configured to model ground mode propagation, as conventional harmonic sources (e.g., industrial facilities, static var compensators, HVDC, etc.) are isolated from the power grid by transformer connections which do not couple the zero sequence; e.g., wye-delta.
- The performance and physical withstand of various power equipment and systems under conditions of extreme harmonic distortion are neither well defined nor adequately documented. Thus, there is difficulty in interpreting the results of a harmonic analysis.

Industrial Experience and the Significance of GMD Harmonics

Harmonic currents and voltages have had major impact on system operations and security during severe GMD events in the past. During the March 1989 geomagnetic storm, the following reported incidents can be reasonably attributed to harmonic distortion created by GIC-saturated transformers [5]:

- Seven static var compensators (SVCs) tripped in rapid succession in the Hydro Quebec system, resulting in system instability and total blackout of that system. Post-event analysis revealed that harmonic distortion was the direct cause of the SVC trips.
- Widespread capacitor banks trips, including 16 bank trips in the Virginia Power system, 12 in the New York Power Pool (predecessor to NYISO), four at Bonneville Power, seven in the Allegheny Power system, and at least three in the PJM system (including 500 kV capacitor banks).
- Generator trips due to negative sequence or phase imbalance protection in the Manitoba Hydro and Ontario Hydro systems (including one major nuclear unit).
- Static var compensator trip in the WAPA system.
- HVDC system trip at the WAPA Miles City station and an HVDC filter trip at the Comerford converter station in the New England system.
- Transmission line trips at Manitoba Hydro and WAPA.

It should be emphasized that only one wide-scale blackout has ever occurred in North America due to GMD, which is the 1989 Hydro Quebec event, and this blackout was clearly initiated by the impact of harmonics.

Report Objectives

This report describes an investigation of the characteristics of harmonic distortion caused by transformers during a GMD, and a scoping assessment of tools needed by the industry to perform an adequate assessment of GMD-related distortion impacts. When the results of a properly performed harmonic assessment are combined with the fundamental frequency analyses, a much more accurate evaluation of grid security during GMD can be obtained.

This report provides technical background and a tutorial discussion on the basics of asymmetric saturation. Harmonic current generation by GIC-saturated transformers is characterized, as well as the relationships of these currents to significant parameters such as GIC magnitude and transformer characteristics. Injection of transformer exciting current into the grid results in voltage distortion, and this voltage distortion affects the generation of harmonics. The non-ideal nature of GIC-saturated transformer harmonic current source characteristics is extensively explored.

Both time-domain and frequency-domain techniques for analysis of GMD-related distortion are assessed. Gaps and shortfalls of presently-available tools for performing GMD harmonic analysis are pointed out, and suggestions are made for future research and tool development.

There are two other topics of importance to GMD-related harmonic distortion assessment that are not addressed in this report. These are:

- Modeling of three-phase transformers and the harmonic currents they produce. Research in this area continues to be active with a number of transformer tests have been initiated in recent years to measure the full harmonic and thermal responses as well as the development of electromagnetic transient transformer models that can be used to derive harmonic current versus GIC relationships [6].
- Following analytic determination of harmonic voltages and currents, the impacts of equipment must be assessed. For some equipment, such as capacitors and generators, existing standards provide sound guidance. For other equipment, such as protective relays, FACTS equipment, and HVDC systems, the vulnerabilities are more complex, specific to designs, and not well defined by existing standards. Guidance for harmonic impact assessment, in the context of GMD events, is not included in this report.

2

TRANSFORMER SATURATION FUNDAMENTALS

Transformer Excitation Curves

The plot of transformer flux versus exciting current is commonly called the “excitation curve” or “saturation curve”. An example is shown in Figure 2-1. Sometimes these curves are plotted in terms of voltage versus exciting current, but it is implied that voltage is fundamental frequency, without distortion and without any flux offset. Given such conditions, per-unit voltage and per-unit flux are equal. Flux is the time integral of voltage, and it is flux that results in transformer saturation.

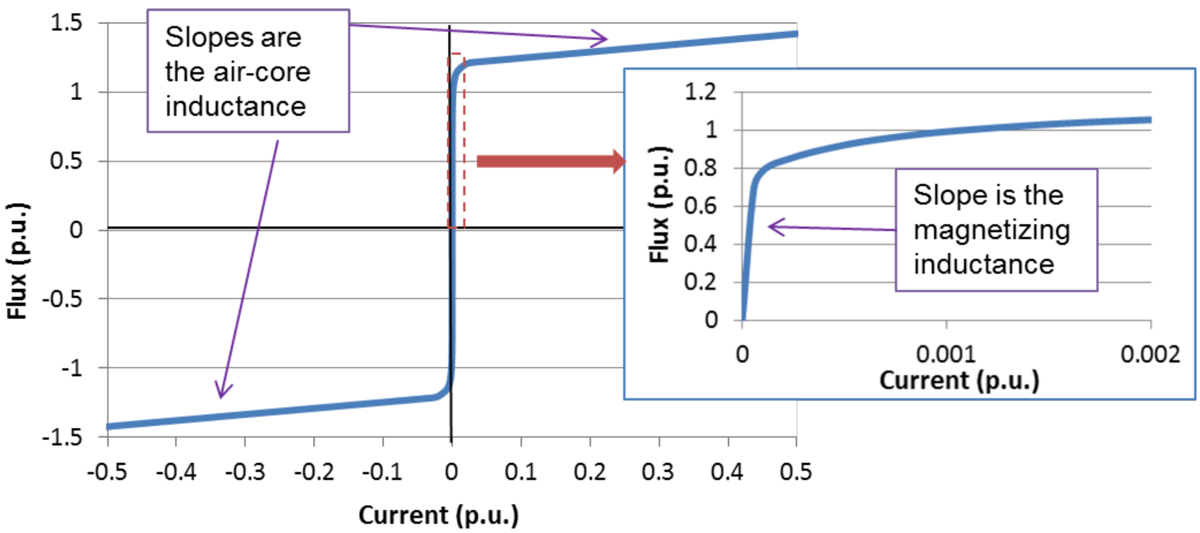

Figure 2-1
Typical power transformer saturation curve

The excitation curve is a function of not only the core material, but also the details of the final core assembly. At flux levels well below the rated peak value, the curve is nearly linear, with a very steep slope. Very little exciting current flows when the flux is at or below the rated value. The slope in this range is known as the magnetizing inductance, and can be on the order of hundreds to thousands of per-unit for a large, high efficiency power transformer. The magnetizing inductance (slope of the curve in the unsaturated region) is determined by both the characteristics of the core steel and the small gaps in the steel at core joints. As the flux level reaches the rated value, the slope or inductance decreases slightly. This is because the flux is concentrated at the joints, and localized saturation begins to occur. For economic reasons, the transformer is designed to operate in this slightly nonlinear range at rated conditions.

Above the range of normal peak flux, the incremental inductance drops off rapidly as the core material begins to saturate over the entirety of the core. Consequently, exciting current increases rapidly. When the core reaches deep saturation, its magnetic permeance approaches that of air. The incremental inductance of the core in deep saturation again becomes linear. This inductance is commonly called the “air core inductance” because it is typically calculated based on the transformer winding configuration alone, as if that winding is suspended in free space (i.e., “air”) without any magnetic core. In reality, the influence of the tank, structural members, and flux shields will make the final slope of the saturation curve slightly greater than the true “air core” inductance. Despite this difference, the common industry usage applies the term “air core inductance” (or impedance) to the final slope of the saturation curve.

If the final slope of the excitation curve is extrapolated back to the flux axis, the flux level at zero current along this line is called the “flux intercept”. Roughly speaking, this is the threshold value of hard saturation.

A transformer excitation curve is symmetrical about the origin, meaning that the behavior is equivalent in both the negative and positive polarities. When the instantaneous flux is plotted against the current for very low-frequency ac excitation, as illustrated in Figure 2-2, a loop is traced. This is caused by hysteresis in the core material, which basically is due to energy required to reverse the magnetic domains. The current where the loop passes the current axis (zero flux) is called the “coercive current”. This current, and thus the width of the “hysteresis” loop, is very small in a modern efficient power transformer. It has almost no relevance to the GIC saturation phenomena discussed in this report and will not be considered further.

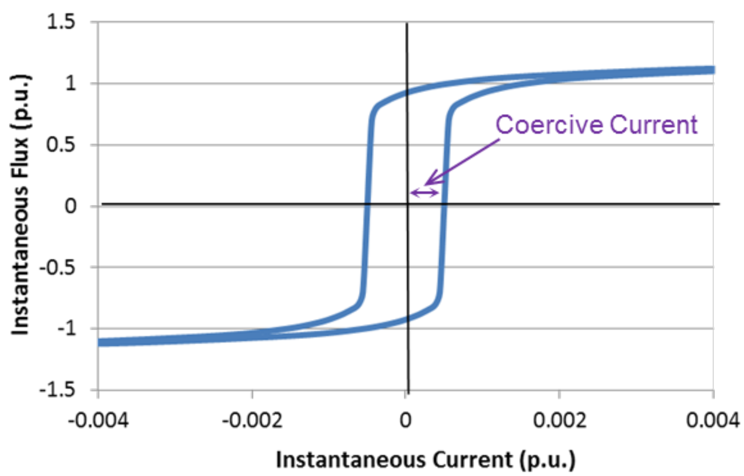

Figure 2-2
Hysteresis loop of a typical power transformer

Symmetric Saturation

Transformers operating at normal levels of fundamental-frequency excitation (e.g., rated voltage at rated frequency, without any direct current) draw an exciting current that is only moderately distorted. This distortion results from the small degree of nonlinearity in the transformer’s flux-current curve within the range of normal flux magnitudes, and hysteresis.

With greater fundamental-frequency excitation, the excitation current rapidly becomes highly distorted. When the flux peaks exceed the level where the entire core leg becomes saturated, the instantaneous excitation current reaches very high levels. With ac overexcitation, the flux peaks exceed both the positive and negative saturation thresholds, resulting in both positive and negative “spikes” of exciting current, as illustrated in Figure 2-3. With undistorted fundamental frequency excitation, and without any flux offset, the exciting current is composed of only odd-order harmonic components.

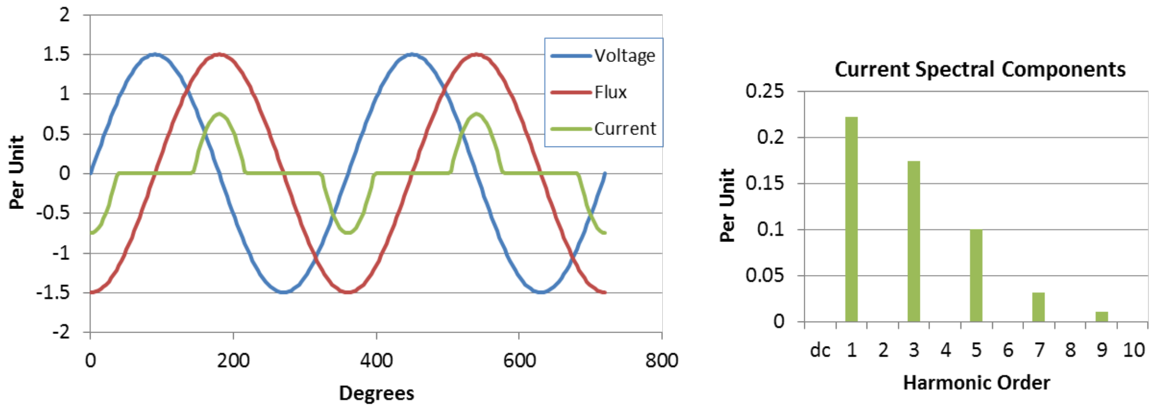

Figure 2-3
Example of symmetric saturation due to overvoltage (flux intercept 1.2 p.u., air-core reactance 0.4 p.u.)

Asymmetric Saturation

Flux can have an offset, or dc value, due to energization of the transformer at other than the voltage crest or with residual flux, or due to direct-current flow through the transformer (e.g., GIC). If there is an offset of the flux, sufficient to cause the transformer's flux to exceed the saturation threshold in only one direction, then the exciting current spikes appear once per cycle and only in one polarity. The components of this exciting current include a fundamental component, even- and odd-order harmonic components, and a dc component. This is illustrated in Figure 2-4.

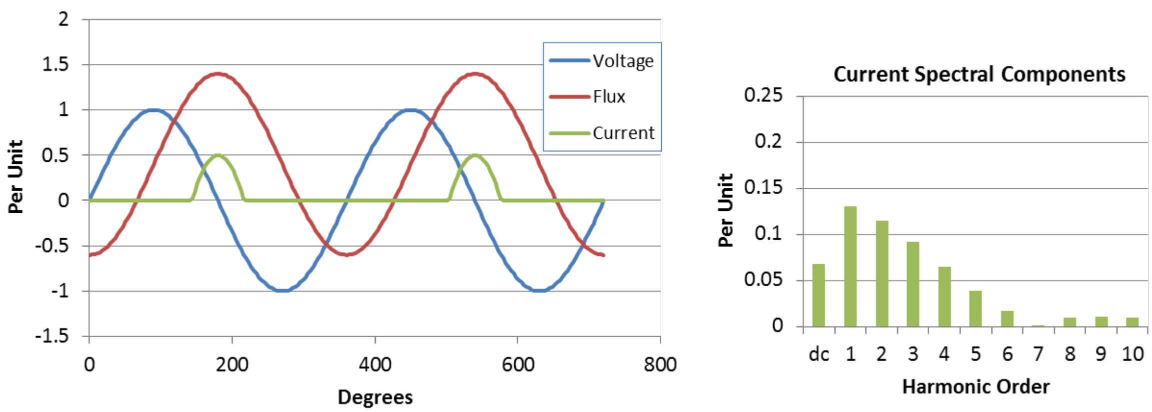

Figure 2-4
Example of asymmetric saturation due to 0.4 p.u. flux offset. (Same transformer as Figure 2-3)

This type of saturation, which can occur even if the applied ac voltage is at the rated value, is termed asymmetric saturation. The term "half-cycle" saturation is also often used to describe the asymmetric saturation caused by GIC. The intended meaning of this term is that saturation takes place on either the positive or the negative half of the cycle, but does not necessarily mean that saturation persists for the entire half cycle. The transformer is not saturated for a full half-cycle, except during very extreme levels of GIC. To avoid misinterpretation, the term "asymmetric saturation" is used instead of "half-cycle saturation" in this report.

Flux Offset Equilibrium

GIC is typically considered as the "cause" for asymmetric saturation during a GMD. However, it is perhaps better to think of the GIC as being allowed to flow as a result of the asymmetric saturation. GIC flow is caused by a quasi-dc voltage induced onto the transmission system. If such a voltage were to begin as a step change, the initial flow of current is not only impeded by the resistance of the transmission system loop (lines, grounded-wye transformers, and substation ground mat resistances), but also by the inductances of the loop. The magnetizing inductance of an unsaturated transformer is very large, and thus the rate of current increase is very slow until the transformer saturates.

Prior to saturation, the dominant inductances of the loop are the transformer magnetizing inductances, which are very large. Initially (time 0+), the dc current is zero and there is no resistive voltage drop. Thus, virtually the entire voltage drop in the loop is initially across the transformer magnetizing inductances (line inductance is insignificant compared to the unsaturated magnetizing inductances of the transformers). Because the flux is the time integral of voltage, the voltage step causes an initial ramp of dc offset in the transformers' fluxes. Until the dc offset causes the flux peaks (offset plus the fundamental sinusoidal peak) to reach the saturation levels of the transformers, the flow of dc increases but is of trivial magnitude. When the flux peaks reach saturation in one polarity, the transformers are in asymmetrically saturation, and their exciting currents begin to have a significant dc component. This dc component causes a dc voltage drop through the loop's resistance, decreasing the dc voltages across the transformers. As a result, the flux offset ramp begins to slow. The ramp rate continues to decrease, and eventually approaches zero when the dc drop across the circuit resistance equals the driving dc voltage. At this point, the dc component of the exciting current is equal to the dc voltage divided by resistance, which is the steady-state GIC magnitude [7]. In essence, the GIC does not begin to flow at a significant magnitude until the transformers saturate. Thus it can be understood that the transformer saturation "allows" the GIC flow, rather than the GIC causing the saturation. The saturation, however, is due to the quasi-dc voltage induced on the transmission lines by the GMD.

Any change of the driving voltage (E-field integrated over distance), or change in the applied ac voltage, results in a similar transient response; the flux offset shifts such that the asymmetric saturation reaches the equilibrium point where the dc component of the exciting current is the GIC. Although the power system response to changing E-field is very slow compared to most power system electromagnetic transients, it is generally faster than variations in the E-field. Therefore, for practical purposes, the GIC can be assumed to be at its steady-state value, which is the driving voltage divided by path resistance. It must be kept in mind, however, that the transformer asymmetric saturation must also be assumed to be at the equilibrium point where the dc component of net exciting current is equal to the net GIC. (Net GIC is the total effective ampere-turns for all of the windings, taking into account the directions of GIC flow in each winding.)

It must be stressed that, because of the nonlinearity of the transformer, superposition cannot be used to separate the ac and dc performance. The dc flux offset is not exclusively set by the amount of GIC. It is necessary for the ac and dc flux to add such that the flux peaks cause sufficient asymmetric saturation for the dc component of the exciting current to be equal to the GIC. If, for example, a transformer with a saturation intercept of 1.2 per unit is passing a small amount of GIC and the ac excitation is one per unit, then the flux offset needs only be slightly more than 0.2 per unit for the equilibrium condition to be reached. If the ac voltage is decreased to 0.9 p.u., the flux offset must increase to greater than 0.3 p.u. to reach the equilibrium.

3 HARMONIC CURRENT INJECTION

The exciting currents of GIC-saturated transformers are highly distorted, and consist of harmonic components of both even and odd orders, as well as fundamental and dc components. In this section, the harmonic currents are characterized and their sensitivities to various parameters are evaluated.

While saturated transformers are commonly thought of as harmonic current sources, the magnitude and phase of the injected current have been found in this research to be significantly affected by distortion of the voltage applied to the transformer. Thus, the transformers cannot be accurately characterized as ideal current sources. The interactions between exciting current harmonic components and harmonic voltage distortion are particularly complex, and are discussed at length in this section. This issue has particular significance to the selection of methodologies and tools used to perform GMD-related harmonic analysis.

Single phase transformers exhibit asymmetric saturation behavior that is far less complex than that of three-phase transformers, due to the lack of magnetic coupling between the phases. Banks of single-phase transformers are commonly used for critical applications, such as EHV autotransformer and major generation step-up transformers, where redundancy is needed for reliability. (It is often more economically efficient to place one single phase transformer as an on-site spare than it is to provide a fully-rated three-phase spare.) EHV autotransformers and GSUs connected to EHV systems tend to have the greatest vulnerability to GIC-related saturation due to the combinations of line lengths as well as line, transformer, and station ground mat resistances characteristic of EHV systems. Single-phase transformers also tend to have the most severe saturation and resulting reactive power demands and harmonic injections, compared to three-phase transformers. Therefore, because single-phase transformers are typically the most critical and most significant, as well as the most straightforward to model and explain, the asymmetric saturation behavior of these transformers is the scope of this report. Future research will be needed to provide similar characterization for three-phase transformers.

Exciting Current Components

Figure 3-1 shows the exciting current components of a single-phase transformer conducting a 0.1 p.u. GIC flow.[1] The fundamental current results in the reactive power demand of the saturated transformer. The second harmonic component is nearly as large as the fundamental, and the magnitudes of the harmonic current components generally tend to decrease with increasing harmonic order. The decreasing trend, however, is not uniform, as the seventh order current is less than the eighth through tenth orders for this transformer at 0.1 p.u. GIC. This plot is for a transformer with an air-core inductance of 0.3 p.u. on its rated voltage and MVA bases. As will

[1] In this report, the per-unit base for GIC is the crest, or peak, value of the rated winding current for the winding conducting the GIC. When a transformer has GIC flow through more than one winding, the net per-unit GIC causing saturation is the sum of the per-unit winding currents respecting the polarity of the GIC flow on each winding (e.g., a 0.1 p.u. GIC flow into one terminal combined with a 0.03 p.u. GIC flow out of another terminal equates to a 0.07 p.u. net GIC flow).

be shown later, the harmonic current components versus GIC are somewhat sensitive to this transformer parameter.

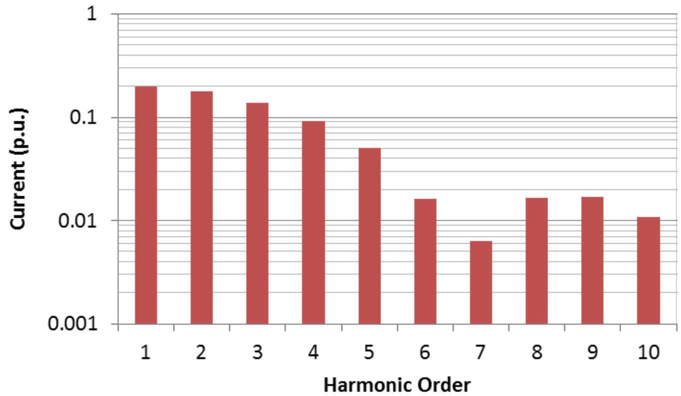

Figure 3-1
Spectral components of exciting current for a transformer passing 0.1 p.u. net GIC

This non-uniform decrease in harmonic component magnitude is also seen when the harmonic current magnitudes are plotted as a function of GIC, as shown in Figure 3-2. Note that the harmonic magnitudes peak and null as the width of the exciting current pulse widens with increasing GIC, and the magnitude cycling becomes more rapid with increasing harmonic order. The apparent discontinuity of the harmonic current magnitude versus GIC plot is actually a continuous oscillation in polarity as show in Figure 3-3. In this plot, the coefficients of the $\cos(n\omega t)$ terms of the Fourier expansion of the exciting current are shown (because the fundamental voltage is defined to be $V_{peak}\cdot\sin(\omega t)$, and thus the flux is $-V_{peak}/\omega\cdot\cos(\omega t)$, the $\sin(n\omega t)$ terms of the Fourier expansion are zero and thus the cosine terms are the magnitudes of the harmonic components).

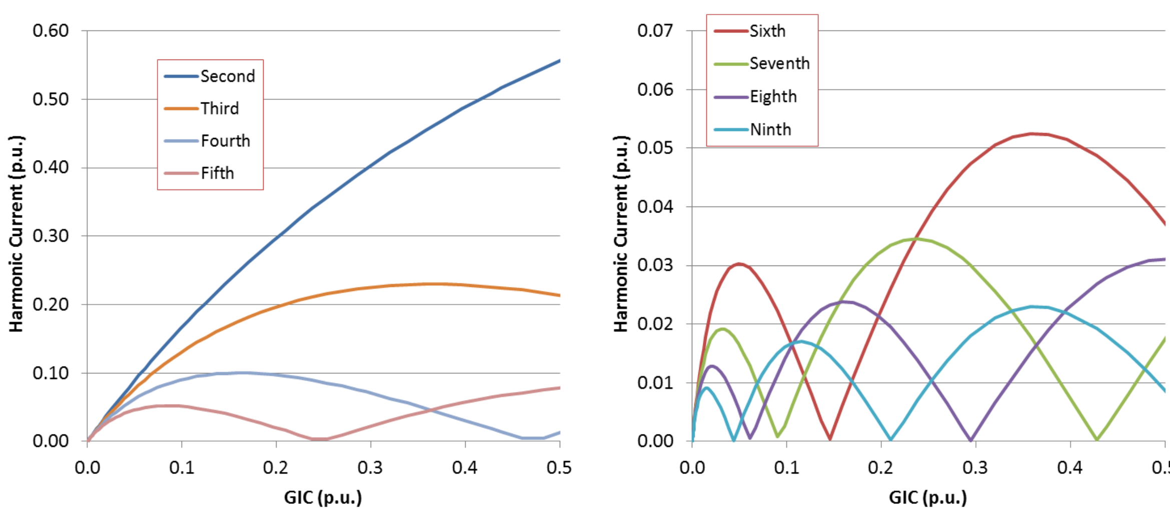

Figure 3-2
Harmonic component magnitudes vs. GIC. (Xac = 0.3 p.u.)

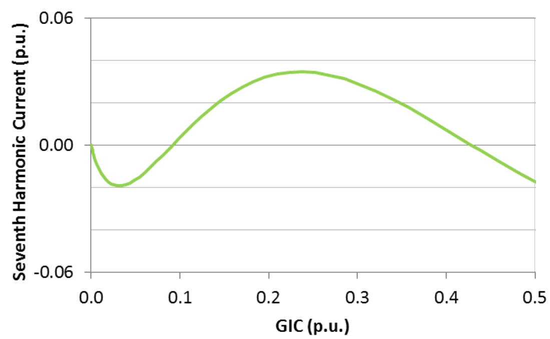

Figure 3-3
Seventh harmonic Fourier cosine term for same conditions as in Figure 3-2.

Analytic Expressions of Harmonic Components

With a simplifying assumption, the fundamental and harmonic exciting current components created by asymmetric transformer can be reduced to analytic equations. The analytical expressions are particularly useful as they directly reveal the sensitivity of the exciting current components to the circuit parameters.

The first critical assumption made for the analytic derivation is that the transformer's saturation curve is a simple characteristic where the exciting current is zero at absolute flux magnitudes less than the saturation level, and the flux versus exciting current follows the air-core inductance slope at flux levels greater than the positive saturation level and less than the negative saturation level. This simplified "single-slope" excitation curve compared with a detailed curve based on typical power transformer characteristics in Figure 3-4. As will be shown later, this simplification of the excitation curve has negligible impact on the harmonic current calculations. The second critical assumption is that the voltage applied to the transformer, and thus the flux, remain undistorted. Effectively, this means that the system is so strong, relative to the transformer, that the exciting current harmonics do not distort the voltage. The impact of voltage distortion on exciting current harmonics will be presented later in this report.

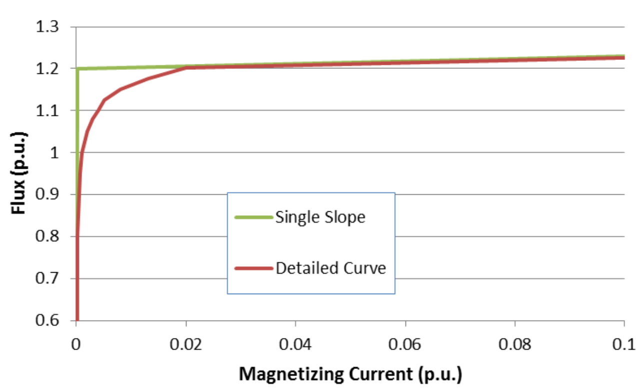

Figure 3-4
Comparison of simplified "single slope" excitation characteristic with a detailed, realistic curve.

Figure 3-5 plots a 1.0 p.u. sine wave of voltage, and the associated cosine flux wave that has a 0.5 p.u. dc offset, such as caused by a GMD. The transformer saturation flux level is assumed to be 1.2 p.u., and the air-core inductance is 0.3 p.u. Because the peak flux exceeds the saturation level by o.3 p.u., the resulting exciting current peaks at 1.0 p.u. The average (dc) value of the exciting current is 0.16 p.u. in this case; thus the net GIC associated with this flux offset condition must necessarily equal 0.16 p.u. The angle from the crest of the applied voltage (and thus the zero point of the ac component of the flux wave, or where the instantaneous flux wave crosses the flux offset level) to the point where the flux reaches the saturation level is defined as α. Given the fundamental voltage magnitude, transformer saturation flux level, and the flux offset, α can be defined as follows:

$$\lambda_s = -\frac{V_p}{\omega}\cos\left(\pi/2 + \alpha\right) + \lambda_0 = \frac{V_p}{\omega}\sin(\alpha) + \lambda_0 \tag{1}$$

V_p/ω can be defined as λ_f, the peak value of the fundamental frequency flux. For a system at nominal frequency, the per-unit magnitude of λ_f is the same as the per-unit magnitude of the applied fundamental voltage.

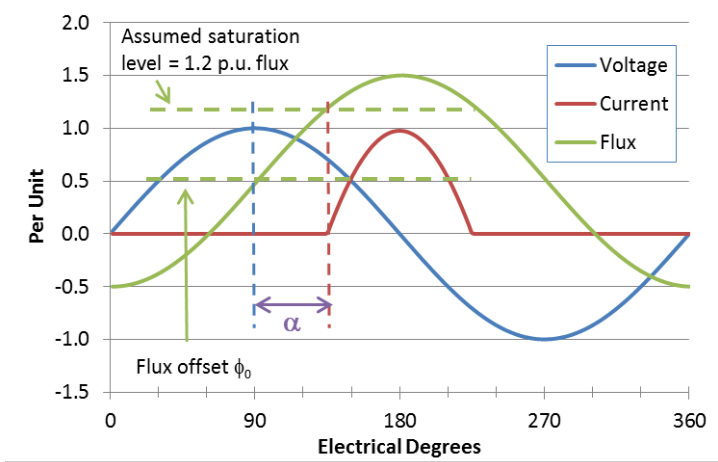

Figure 3-5
Voltage, flux with 0.5 p.u. offset, and exciting current

Solving for α:

$$\alpha = Sin^{-1}\left(\frac{\lambda_s - \lambda_0}{\lambda_f}\right) \tag{2}$$

As discussed in the previous section, circuit equilibrium conditions require that the transformer flux offset is such that the dc component of the exciting current is equal to the conducted net GIC. From the derivation detailed in Appendix A.1, the GIC is related to α, the applied fundamental-frequency voltage peak magnitude $V_{p,}$ and the transformer air-core reactance X_{ac} by Equation (3).

$$i_{GIC} = \frac{1}{2\pi}\cdot\frac{V_p}{X_{ac}}\left[2\cdot\cos(\alpha) - \pi\cdot\sin(\alpha) + 2\alpha\cdot\sin(\alpha)\right] \tag{3}$$

Because this equation is transcendental, iteration must be used to solve for α. If the GIC is expressed in per-unit on the base of the transformer winding's rated peak (crest) current, as recommended in the previous section of this report, then this equation can be expressed in per-unit as follows:

$$\bar{i}_{GIC} = \frac{1}{2\pi} \cdot \frac{\overline{V}_f}{\overline{X}_{ac}} \left[2 \cdot \cos(\alpha) - \pi \cdot \sin(\alpha) + 2\alpha \cdot \sin(\alpha) \right] \tag{4}$$

From the derivation detailed in Appendix A.2, the fundamental (reactive) exciting current component can be defined, in per-unit, as:

$$\bar{i}_f = \frac{\overline{V}_f}{2\pi \cdot \overline{X}_{ac}} \cdot \left[2\alpha - \pi + \sin(2\alpha) \right] \tag{5}$$

In this equation, V_f is the per-unit fundamental voltage, and the per-unit air core reactance is on the same MVA and voltage bases as used to define the per-unit base for the GIC.

The rather complicated derivation of harmonic exciting current components versus α is detailed in Appendix A.3. The cos($n\omega t$) current components for GIC flow into the transformer (from terminal to ground), where n is the harmonic order or per-unit frequency, are:

$$\bar{i}_n = \frac{\overline{V}_f}{\pi \cdot \overline{X}_{ac}} \cdot \left[-\frac{\cos\left(n\pi/2 + (n-1)\cdot\alpha\right)}{n-1} + \frac{\cos\left(n\pi/2 + (n+1)\cdot\alpha\right)}{n+1} + 2 \cdot \frac{\sin(\alpha)}{n} \cdot \sin\left(n \cdot \left(\pi/2 + \alpha\right)\right) \right] \tag{6}$$

With the applied voltage defined to be $V_p \cdot \sin(\omega t)$, all of the harmonic magnitudes are defined by the cos($n\omega t$) terms and all the sin($n\omega t$) terms are equal to zero.

Validation of Simplified Excitation Characteristic Approximation

The validity of assuming the simplified transformer excitation characteristic can be evaluated by comparing time-domain simulations of the exciting currents, using a detailed excitation curve, with the results of the analytic calculations. Figure 3-6 compares the second and fifth harmonic current components versus GIC. As is shown in this figure, the magnitudes of the harmonic current components are, for all practical purposes, essentially equal. Thus, the asymmetric saturation behavior is very independent of the details of the single-phase transformer saturation characteristics, other than the air-core inductance. This validates the critical assumption on which the derivations of the analytic expressions are based.

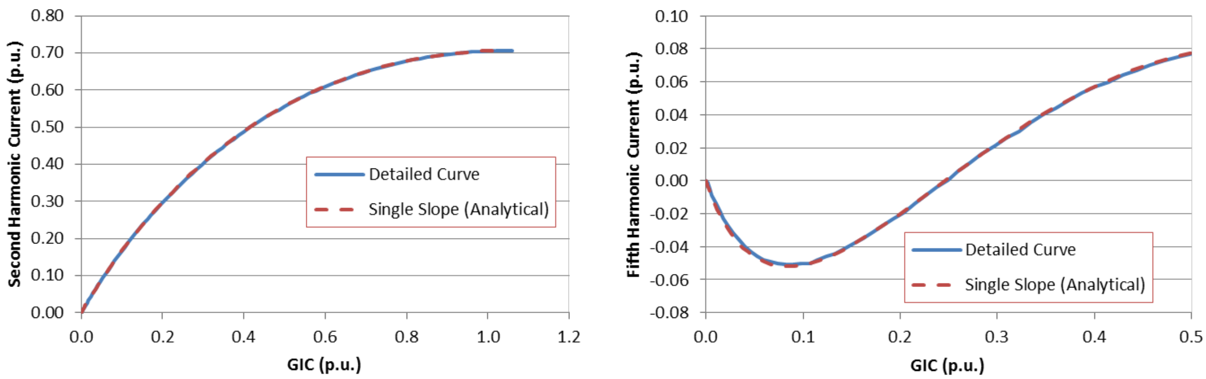

Figure 3-6
Comparison of harmonic components vs. GIC determined by analytic calculation using a simplified excitation characteristic (single-slope) and by time-domain simulation using a detailed, realistic excitation curve.

Parametric Sensitivities

GIC Flow Direction Sensitivity

Because the average value of the exciting current must equal the effective GIC in the steady state, the polarity of the asymmetric exciting current pulse is dictated by the net GIC polarity. An inherent characteristic of semi-sinusoidal (half-wave) pulses is that the odd harmonic frequency components are invariant with pulse polarity, but the even harmonic components have polarities that reverse with a reversal of the pulse polarity. While a derivation similar to that documented in Appendix A.3 , not included in this report, can be made for GIC flow out of the transformer (from ground to terminal), the sensitivity of the exciting current components to GIC polarity can also be evaluated by time-domain simulation, as was used to produce the results discussed below.

Figure 3-7 compares the dc and cos($n\omega t$) current components for positive and negative flux offset for a transformer with a 1.2 p.u. flux intercept (saturation level) and 0.4 p.u. air core impedance, with an applied 1.0 p.u. fundamental frequency voltage. Note that the positive dc component, resulting from the positive flux offset, indicates a GIC flow into the transformer, and the negative dc component for the case with negative flux offset indicates GIC flow out of the transformer. The magnitudes of the dc, fundamental, and harmonic currents are invariant with offset polarity, as are the polarities of the fundamental and odd-order harmonic components. The even-order components, however, reverse polarity when the flux offset polarity is reversed. Because the dc component of the exciting current is equal in magnitude and polarity with the GIC, it can be seen that the polarities of even-order harmonic components are a function of GIC flow direction, while odd orders are not.

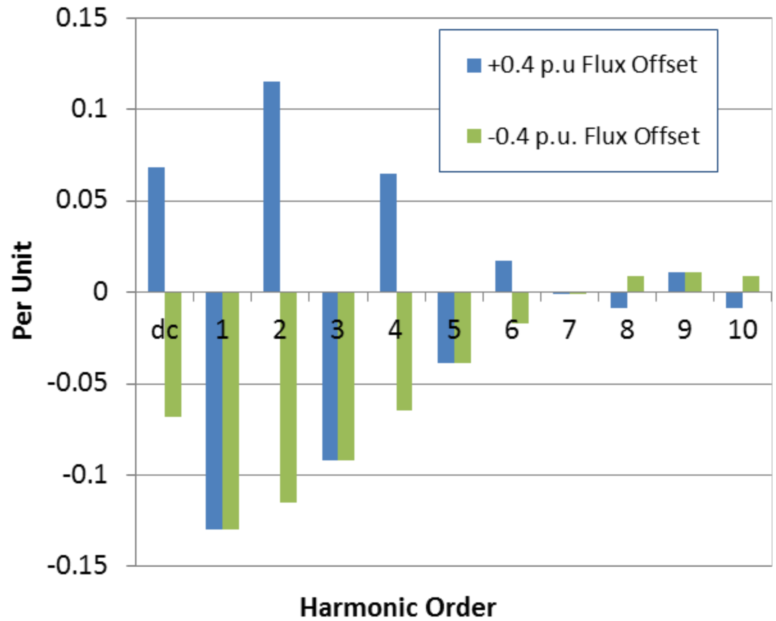

Figure 3-7
Comparison of exciting current component polarities for positive and negative flux offset.

A generalized equation for the harmonic components is:

$$\bar{i}_n = \frac{\overline{V}_f}{\pi \cdot \overline{X}_{ac}} \cdot \left[-\frac{\cos\left(n\pi/2 + (n-1)\cdot\alpha\right)}{n-1} + \frac{\cos\left(n\pi/2 + (n+1)\cdot\alpha\right)}{n+1} + 2 \cdot \frac{\sin(\alpha)}{n} \cdot \sin\left(n \cdot \left(\pi/2 + \alpha\right)\right) \right] \cdot \left(k_{GIC}\right)^{n+1} \quad (7)$$

where k_{GIC} is +1 for flow into the transformer and -1 out of the transformer.

Relationship to Fundamental Voltage Phase Angle

When the phase angle of the fundamental voltage applied to the transformer is shifted from zero, i.e., the voltage is defined as $V(t) = V_p \cdot \sin(\omega t + \Phi)$, there is also a shift in the phase of the exciting current components relative to the absolute reference. Table 3-1 compares the harmonic component phasors for fundamental voltage angles of zero and ±10 degrees, with GIC flow in and out of the transformer. In all cases in this table, the GIC magnitude is 0.1 p.u., the applied voltage is 1.0 p.u., and the air-core reactance is 0.3 p.u. It can be seen that for a shift of the fundamental angle Φ, the absolute phase angle of the harmonic components is shifted by n·Φ.

Table 3-1
Exciting Current Component Magnitude and Phase Angles for Various Fundamental Phase Angles and GIC Flow Directions.

Order	$\lvert I_{exc} \rvert$	I_{exc} Component Phase Angles					
		$\angle V_{fund} = 0°$		$\angle V_{fund}$=+10°		$\angle V_{fund}$=-10	
		I_{GIC}=+0.1	I_{GIC}=-0.1	I_{GIC}=+0.1	I_{GIC}=-0.1	I_{GIC}=+0.1	I_{GIC}=-0.1
1	0.191	-90°	-90°	-80°	-80°	-100°	-100°
2	0.167	90°	-90°	110°	-70°	70°	-110°
3	0.131	-90°	-90°	-60°	-60°	-120°	-120°
4	0.09	90°	-90°	130°	-50°	50°	-130°
5	0.051	-90°	-90°	-40°	-40°	-140°	-140°
6	0.019	90°	-90°	150°	-30°	30°	-150°
7	0.004	90°	90°	160°	160°	20°	20°
8	0.015	-90°	90°	-10°	170°	-170°	10°
9	0.016	90°	90°	180°	180°	0°	0°
10	0.012	-90°	90°	10°	-170°	170°	-10°

From the observed relationships between fundamental voltage phase angle and GIC flow polarity, a generalized phasor expression for exciting current harmonic components for transformers conducting GIC is:

$$\tilde{\bar{I}}(h) = \left| \frac{\bar{V}}{\bar{X}_{ac}} \right| \cdot W(h,\alpha) \angle \left(-90° \cdot \left(k_{GIC} \right)^{h+1} + h \cdot \phi \right) \tag{8}$$

Where:

$$W(h,\alpha) \equiv \left| \frac{1}{\pi} \cdot \left[-\frac{\cos\left(n\pi/2 + (n-1)\cdot\alpha \right)}{n-1} + \frac{\cos\left(n\pi/2 + (n+1)\cdot\alpha \right)}{n+1} + 2 \cdot \frac{\sin(\alpha)}{n} \cdot \sin\left(n \cdot \left(\pi/2 + \alpha \right) \right) \right] \right| \tag{9}$$

As previously indicated, k_{GIC} is +1 for flow into the transformer and -1 for flow out.

For single-phase transformer, the saturation behavior is sufficiently simple that the harmonic magnitudes can be defined by analytic expressions. The complicated inter-phase magnetic coupling of three-phase transformers, however, makes derivation of analytic expressions for these transformers infeasible.

Fundamental Voltage Magnitude Sensitivity

Figure 3-8 plots the variation in harmonic component magnitudes as a function of the magnitude of the fundamental voltage applied to the transformer. In this figure, the air-core impedance is 0.3 p.u. and the GIC flow is 0.1 p.u. into the transformer. The lower-order harmonics are relatively invariant over a reasonable fundamental voltage magnitude range. There is a modest degree of variability in the higher order harmonic magnitudes (sixth harmonic and higher).

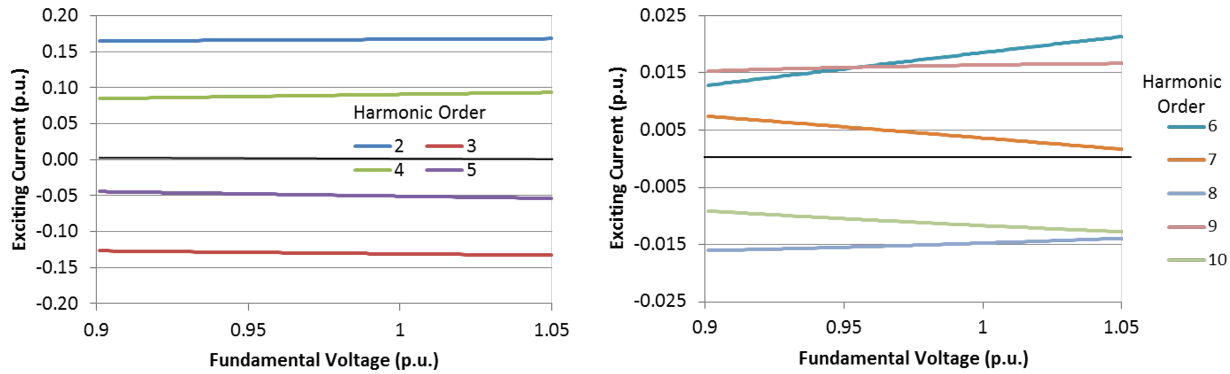

Figure 3-8
Exciting current harmonic component sensitivity to fundamental voltage, at 0.1 p.u. GIC

Air-Core Inductance Sensitivity

Exciting current harmonic component magnitudes and polarity are quite sensitive to the transformer's air-core reactance, particularly at the higher harmonic orders and at higher levels of GIC, as shown in Figure 3-9 to Figure 3-11. The transformer air-core reactance is 0.3 p.u. in all of these plots.

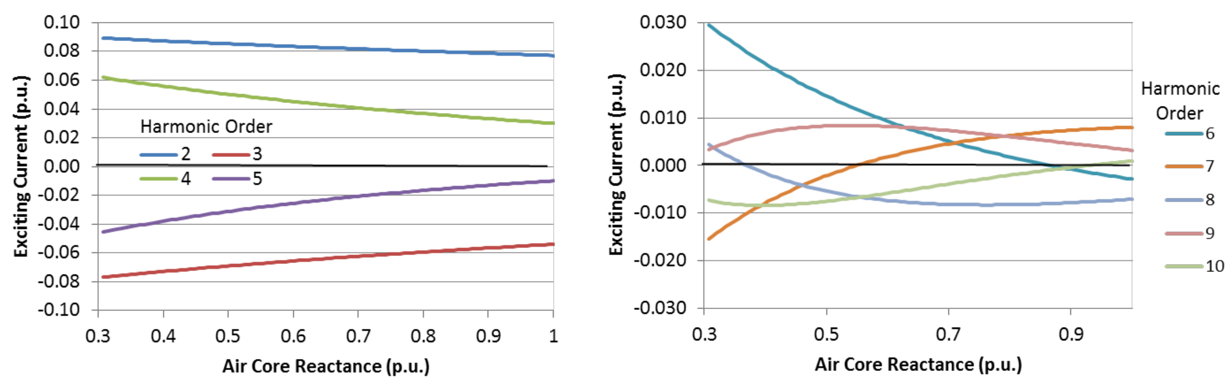

Figure 3-9
Sensitivity of exciting current harmonic components to air-core reactance. (GIC= 0.05 p.u.)

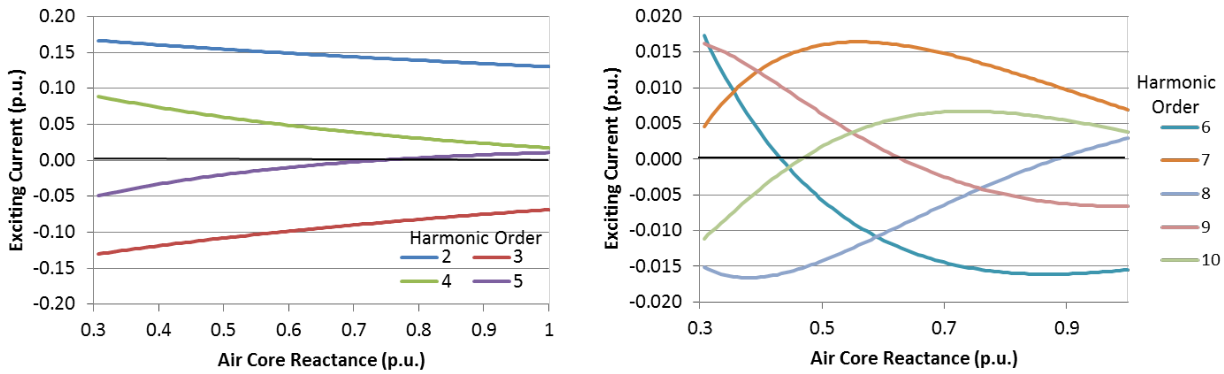

Figure 3-10
Sensitivity of exciting current harmonic components to air-core reactance. (GIC= 0.1 p.u.)

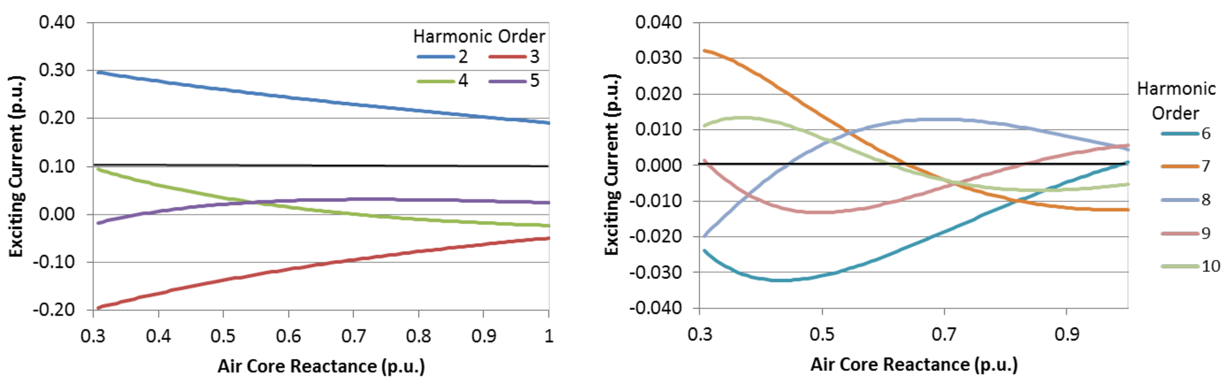

Figure 3-11
Sensitivity of exciting current harmonic components to air-core reactance. (GIC= 0.2 p.u.)

Air-core impedance is not a transformer nameplate datum, and is typically not included with the transformer test information that a transformer purchaser is routinely provided. This parameter, however, can often be obtained from the transformer manufacturer on request. While the range of power transformer air-core impedances spans from approximately 0.3 p.u. to 1.0 p.u., the ranges are more limited for particular design types. Core-form designs tend to have lower air-core impedances, generally in the 0.3 to 0.5 p.u. range. Shell-form designs tend to have air-core impedances at the upper end of the plotted range, typically in the range of 0.8 to 1.0 p.u. Thus, a reasonable estimate of transformer air-core reactance can be made if the basic transformer design type is known.

Impact of Voltage Distortion on Current Injection

The illustrations of harmonic exciting current shown previously in this report were all based on the assumption of an undistorted fundamental-frequency voltage applied to the transformer. Unless a system is infinitely strong, however, the harmonic currents injected by a transformer will interact with the system's driving point harmonic impedances to create harmonic voltages. During a GMD, harmonic currents injected by other transformers subjected to GIC flow will also contribute. Although saturated transformers are often viewed as ideal harmonic current sources, this is a very simplistic assumption that becomes increasingly inaccurate as the distortion of the voltage applied to a transformer increases.

To illustrate, Figure 3-12 shows voltage, flux, and current for an ideal situation where the voltage is completely undistorted. In Figure 3-13, a 0.2 p.u. fourth harmonic "in-phase", or direct axis, voltage component is superimposed on the fundamental. By "in phase", it is meant that the fourth harmonic voltage is superimposed as a sine function onto the fundamental, which is also expressed as a sine function. Described mathematically, the voltage, as a function of time, is the expression shown in the bottom of the figure. Comparing Figure 3-12 with Figure 3-13, the added voltage distortion, distorts the flux waveform, and as a result, the exciting current pulse is broadened and shortened. This changes the spectral content of the exciting current.

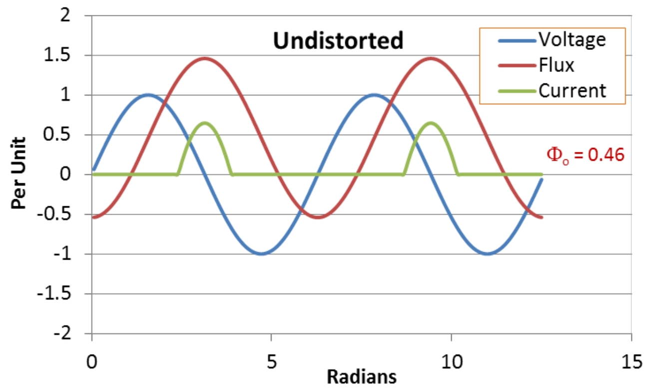

Figure 3-12
Illustration of transformer exciting current produced by offset saturation with undistorted fundamental voltage applied.

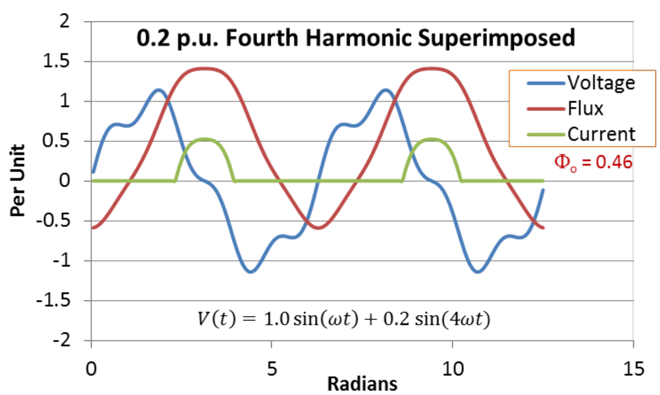

Figure 3-13
Same conditions as Figure 3-12 except that a 0.2 p.u. fourth harmonic voltage is superimposed.

In Figure 3-14, the same magnitude of fourth harmonic voltage is superimposed, but with a phase angle leading by 90° relative to the fourth harmonic voltage that was superimposed on the fundamental Figure 3-13. The qualitative impacts of the phase shift in the distortion on the exciting current waveform can be clearly seen. The exciting current pulses are narrower and taller than in the prior two cases.

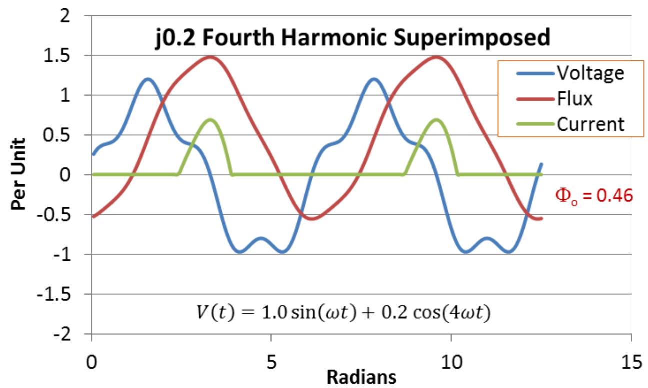

Figure 3-14
Same conditions as Figure 3-13 except that the phase angle of the superimposed fourth harmonic voltage leads by 90°.

The impacts of the voltage distortion on the spectral content of the exciting current are shown in Figure 3-15 and Figure 3-16. It can be observed that the applied distortion changes the exciting current components at not only the harmonic order (frequency) of the applied voltage distortion, but at almost every other harmonic order as well. There is also a small amount of sensitivity of the fundamental (harmonic order 1) current to distortion. This means that the fundamental frequency reactive power demand imposed by a GIC-saturated transformer is slightly affected by the interaction of the transformer (and other transformers in the system) with the system's harmonic impedances. The largest relative and absolute changes can occur at frequencies other than the voltage distortion frequency; note the fifth harmonic changes more than the fourth harmonic for superposition of a real fourth harmonic voltage component. The changes in exciting current harmonic phase angles are far more profound at some frequencies than the changes in absolute magnitudes.

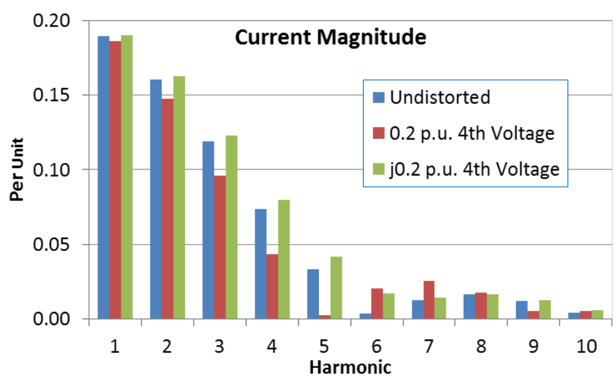

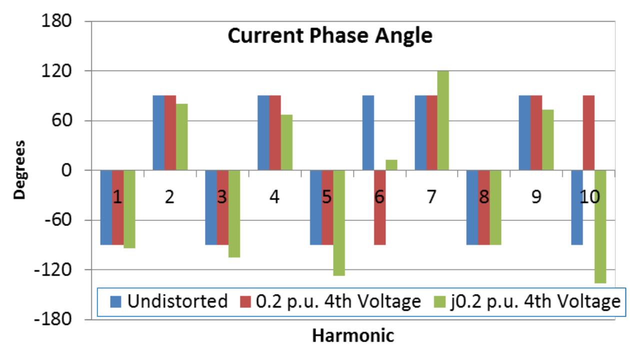

Figure 3-15
Comparison of exciting current harmonic component magnitudes and phase angles for distorted and undistorted voltage applied to the transformer.

The impact of voltage distortion on exciting current harmonic component phase angle is perhaps better illustrated by considering the exciting current harmonics plotted as real and imaginary components as shown for the same cases in Figure 3-16. Real components are the Fourier sine term coefficients, when the applied fundamental voltage is a sine wave. Imaginary terms are 90° leading, or cosine terms. Without voltage distortion, or with real harmonic voltage distortion applied, the exciting current components are all imaginary terms. Real voltage component distortion causes some change in the exciting current imaginary components, but the real harmonic components remain zero. If an imaginary voltage distortion component is superimposed, real current harmonic components appear, but the imaginary components remain the same as the undistorted case.

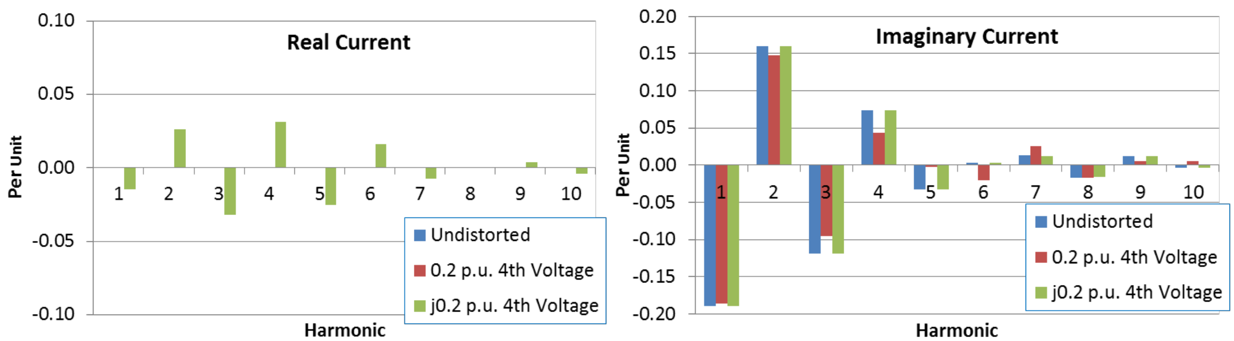

Figure 3-16
Comparison of exciting current harmonic real and imaginary component magnitudes for distorted and undistorted voltage applied to the transformer.

Harmonic-Space Admittance Matrix

A current source that is non-ideal, meaning its current output is a function of the voltage into which it is driving, can usually be represented as a Norton equivalent source; i.e., a current source in parallel with an admittance. In the case of the GIC-saturated transformer, the harmonic orders are cross-coupled, due to the nonlinearity of the transformer. Currents at one frequency are a function of voltages at all frequencies. A "harmonic space" admittance matrix can be used to describe such a cross-coupled source. The terms of such a matrix are defined in Equation (10), with *k* and *m* denoting harmonic orders.

$$Y_{k,m} = \frac{\Delta I_k}{\Delta V_m} \tag{10}$$

The response of the transformer, however, is different for voltage distortion perturbations with real components (d-axis distortions) and imaginary components (q-axis distortions). In other words, a 90° shift in the voltage distortion phase angle does not just result in a 90° shift in the resulting current, but there is also a magnitude change. Therefore, the resulting change in exciting current for a voltage distortion $V = V_d + jV_q$ is:

$$\Delta I = Y_d \cdot V_d + jY_q \cdot V_q \tag{11}$$

where:

$$Y_{d\,k,m} = \frac{\Delta I_k}{\Delta V_{d\,m}} \qquad Y_{q\,k,m} = \frac{\Delta I_k}{\Delta V_{q\,m}} \tag{12}$$

For an example case of a single-phase transformer with an air-core reactance of 0.4 p.u. passing 0.1 p.u. GIC and with 1.0 p.u. fundamental voltage applied, the Y_d and Y_q harmonic space admittance matrix terms are shown in Table 3-2 and Table 3-3, respectively. The terms of these matrices were created using small (0.01 p.u.) voltage distortion perturbations.

Table 3-2
Direct Axis Harmonic Space Matrix

Y_d	1	2	3	4	5	6	7	8	9	10
1	-0.01*j	0.011*j	-0.017*j	0.015*j	-0.011*j	0.008*j	-0.004*j	0.00	0.002*j	-0.003*j
2	0.027*j	-0.043*j	0.056*j	-0.054*j	0.043*j	-0.029*j	0.013*j	0.00	-0.008*j	0.01*j
3	-0.047*j	0.081*j	-0.102*j	0.1*j	-0.083*j	0.056*j	-0.027*j	0.003*j	0.012*j	-0.016*j
4	0.06*j	-0.108*j	0.134*j	-0.135*j	0.115*j	-0.08*j	0.043*j	-0.01*j	-0.01*j	0.018*j
5	-0.061*j	0.11*j	-0.138*j	0.143*j	-0.127*j	0.095*j	-0.058*j	0.024*j	0.00	-0.011*j
6	0.046*j	-0.087*j	0.111*j	-0.121*j	0.114*j	-0.095*j	0.069*j	-0.042*j	0.019*j	-0.003*j
7	-0.022*j	0.044*j	-0.061*j	0.075*j	-0.081*j	0.08*j	-0.072*j	0.058*j	-0.041*j	0.024*j
8	-0.003*j	0.002*j	0.006*j	-0.021*j	0.039*j	-0.056*j	0.067*j	-0.068*j	0.059*j	-0.043*j
9	0.022*j	-0.036*j	0.037*j	-0.023*j	-0.001*j	0.029*j	-0.053*j	0.067*j	-0.068*j	0.057*j
10	-0.028*j	0.048*j	-0.054*j	0.045*j	-0.023*j	-0.006*j	0.034*j	-0.054*j	0.063*j	-0.06*j

Table 3-3
Quadrature Axis Harmonic Space Matrix

Y_q	1	2	3	4	5	6	7	8	9	10
1	-0.19*j	0.16*j	-0.119*j	0.074*j	-0.033*j	0.004*j	0.013*j	-0.017*j	0.012*j	-0.004*j
2	0.321*j	-0.273*j	0.205*j	-0.131*j	0.063*j	-0.013*j	-0.016*j	0.025*j	-0.019*j	0.008*j
3	-0.357*j	0.308*j	-0.237*j	0.159*j	-0.087*j	0.031*j	0.004*j	-0.019*j	0.018*j	-0.01*j
4	0.295*j	-0.261*j	0.212*j	-0.156*j	0.101*j	-0.054*j	0.02*j	0.00	-0.008*j	0.008*j
5	-0.166*j	0.158*j	-0.145*j	0.126*j	-0.103*j	0.077*j	-0.051*j	0.028*j	-0.009*j	-0.003*j
6	0.021*j	-0.039*j	0.062*j	-0.082*j	0.093*j	-0.091*j	0.077*j	-0.055*j	0.03*j	-0.008*j
7	0.088*j	-0.056*j	0.01*j	0.036*j	-0.072*j	0.09*j	-0.09*j	0.073*j	-0.048*j	0.022*j
8	-0.132*j	0.098*j	-0.05*j	-0.001*j	0.044*j	-0.073*j	0.084*j	-0.078*j	0.06*j	-0.037*j
9	0.108*j	-0.087*j	0.055*j	-0.018*j	-0.017*j	0.044*j	-0.062*j	0.067*j	-0.062*j	0.049*j
10	0.041*j	0.038*j	-0.032*j	0.021*j	-0.006*j	-0.013*j	0.031*j	-0.046*j	0.055*j	-0.055*j

Admittance Matrix Sensitivities and Linearity

To be of value in a potential GIC harmonic analysis algorithm, the admittance matrices should be relatively invariant with the voltage distortion magnitude. Figure 3-17 plots the coefficients of the Y_d column as a function of second harmonic distortion magnitude. The results indicate that the matrix terms are relatively constant, indicating piece-wise linearity. Figure 3-18 plots the same matrix coefficients versus the GIC magnitude. It can be seen that the coefficients vary nearly linearly with the GIC magnitude. This implies that it may be possible to develop harmonic-space Norton admittance matrices for a particular transformer, where the coefficients are a predictable function of GIC magnitude. The exploitation of this approach to develop an algorithm useful for analyzing GIC-related harmonic distortion is beyond the scope of this project.

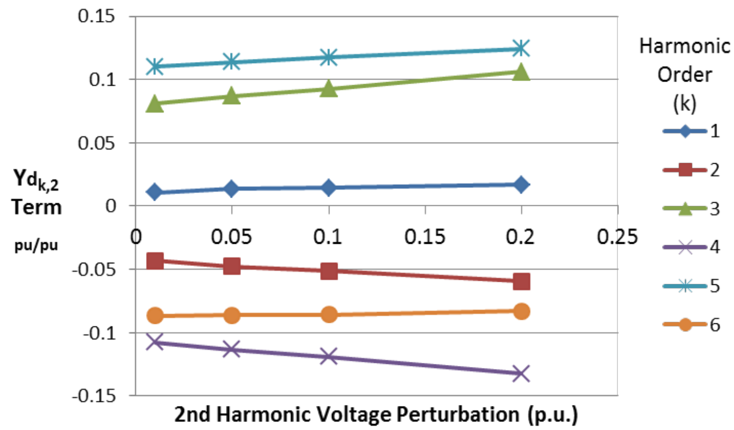

Figure 3-17
Sensitivity of d-axis harmonic-space Norton source admittance matrix second-column terms to magnitude of second harmonic voltage perturbation.

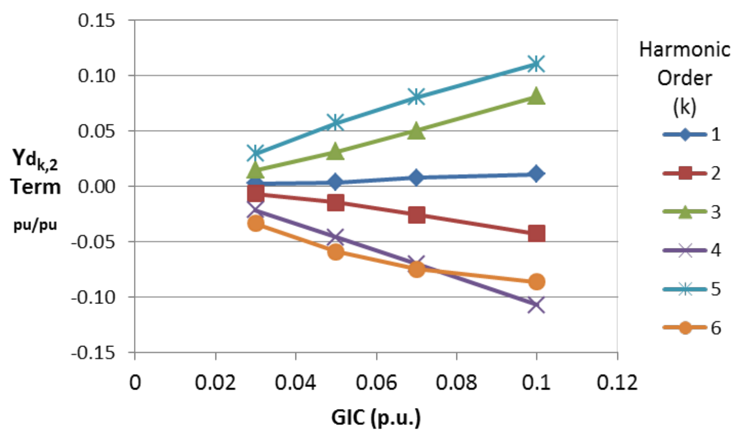

Figure 3-18
Sensitivity of d-axis harmonic-space Norton source admittance matrix second-column terms to GIC magnitude.

4

ITERATIVE ANALYSIS OF GMD-RELATED DISTORTION

As discussed previously in this report, the harmonic currents injected into a power system by a GIC-saturated transformer will interact with the system impedances to produce voltage distortion. This distortion will, in turn, affect the magnitude and phase angle of the injected harmonic current. Although future research might develop a direct analysis approach using Norton equivalent sources and harmonic-space admittance matrices, other more conceptually-simple approaches can be used instead. When dealing with large systems, however, these alternate approaches could be computationally burdensome.

Iterative Analysis Algorithm

Single-Transformer Algorithm

Described below is an iterative approach to analysis of harmonic distortion caused by a single GIC-saturated transformer, including the interaction between voltage distortion and exciting current:

1. Perform dc GIC flow analysis.
2. Initially assume that the applied fundamental-frequency voltage is undistorted and of nominal (1.0 p.u.) magnitude.
3. Calculate the saturation delay angle α using Equation (4). Because this equation is transcendental, α cannot be determined directly, but must be found using iteration.
4. Using the determined value of α, calculate the fundamental reactive current demand of the transformer using Equation (5).
5. Assume the transformer to be a constant reactive current load and solve for the fundamental-frequency voltage at the transformer terminals.
6. If the voltage magnitude at the transformer is different than found in Step 5, return to Step 3 using the new fundamental voltage magnitude estimate and continue iterating through Steps 3 – 6 until convergence is achieved. (The transformer is close to, but not precisely equal to a constant-current fundamental-frequency load.)
7. Calculate the harmonic current injection phasors using the solved fundamental-frequency voltage magnitude and angles, as well as the calculated α as inputs.
8. Calculate the transformer voltage distortion at each harmonic frequency using these harmonic currents injected into the system driving point harmonic impedances.
9. The frequency-domain flux is calculated by dividing the voltage magnitudes by the angular frequency of each component, shifting each voltage harmonic component phase angle by -90°, and adding a dc flux bias (which can initially be calculated using Equation (13)).

$$\lambda_o = \lambda_s - \frac{\overline{V}_f}{\overline{\overline{X}}_{ac}}(\sin\alpha) \tag{13}$$

10. Convert the resulting frequency-domain into a time-domain flux waveform.
11. The time-domain flux waveform is then applied to the nonlinear current versus flux characteristic of the transformer to obtain the time-domain exciting current.
12. Fourier analysis of the time-domain exciting current yields the exciting current harmonic components and the dc component.
13. The dc component is compared with the net GIC. If unequal, the flux offset λ_o is adjusted and the process returns to Step 9, iterating steps 9 - 12 until the value of the dc component of the exciting current is equal to the net GIC. When the flux offset has converged, the harmonic current magnitudes and phase angles are compared to the harmonic currents used in Step 8. If not sufficiently equal, return to Step 8 using the new harmonic currents found in Step 12 for the solved value of flux offset. Repeat Steps 8-13 until the harmonic current magnitude and phase angles converge. The exciting current is re-calculated and this iterative loop continues until the dc component of the exciting current converges to the GIC magnitude.
14. After dc convergence, the harmonic components of exciting current are again injected into the driving point impedance to obtain a new estimate of the terminal voltage distortion. (Return to Step 8.) The iterative process is continued, including the sub-loop where flux offset is iterated, until the harmonic current components used in Step 8 are sufficiently equal to those found in Step 12. I.e., current harmonic convergence is achieved.

In cases with very high GIC, or with very high system harmonic impedances (such as caused by lightly-damped resonance at a harmonic frequency), the iterative process may diverge. Other, more sophisticated iterative approaches may be needed to achieve convergence.

Experience has shown that the fundamental current is not significantly affected by the harmonic voltage distortion, if the flux offset is adjusted such that the dc component of the exciting current remains equal to the GIC (i.e., flux offset equilibrium condition is maintained). Therefore, the algorithm described above does not loop back from the harmonic solution to the fundamental-frequency voltage solution. However, a more exact analysis algorithm would do so.

Multi-Transformer Algorithm

In a realistic power system during GMD, many transformers are likely to be saturated concurrently. The harmonic currents injected by one transformer are very likely to affect the voltage distortion present at another transformer. The multi-transformer iterative analysis is more complex because the voltage distortion at each transformer must include the distortion contributions of every other transformer, with careful consideration of relative phasing. The phase angle of the harmonic voltage contribution from a remote transformer is a function of:

- GIC magnitude and polarity through the remote transformer.
- Remote transformer characteristics (for single-phase transformers, only the air-core impedance is of importance).
- Fundamental frequency voltage magnitude and phase angle at the remote transformer
- Voltage distortion at the remote transformer
- Harmonic transfer impedance angle

Therefore, the iterative solution in a multi-transformer case must consider all of these factors related to harmonic current phase in an algorithm very similar to that described for the single-transformer situation. Because the fundamental voltage magnitude and angle are governed by loadflow constraints, the iterative harmonic analysis program should be linked to a loadflow algorithm. Figure 4-1 shows a block diagram of the iterative algorithm for large-system GMD harmonic analysis. Unfortunately, there is no known software tool presently available on a commercial basis with the capability to perform this analysis.

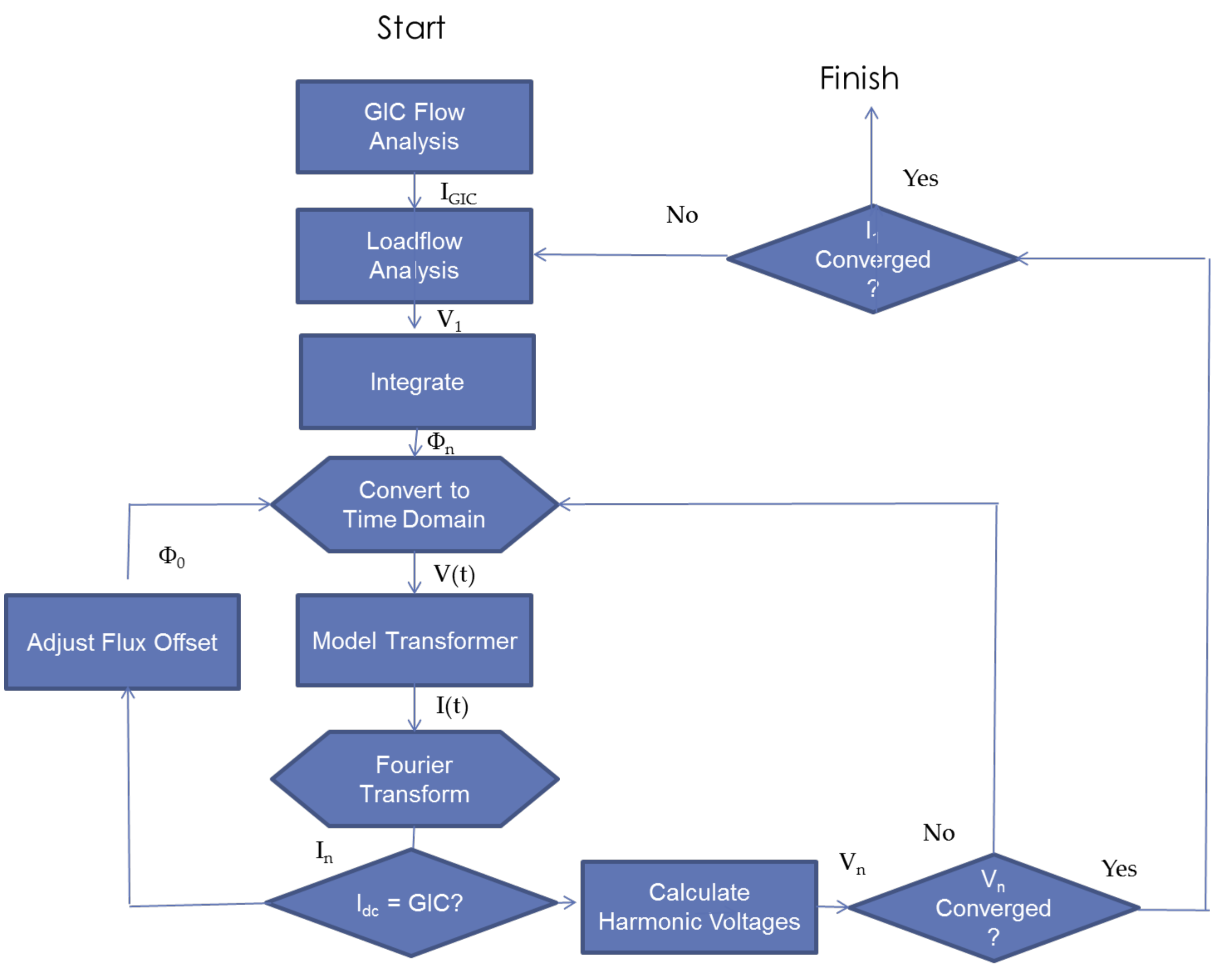

Figure 4-1
Iterative process for system analysis of harmonics during GMD

Comparison of Solved and Single-Pass Distortion Results

The significance of closed-loop harmonic distortion interaction with GIC-saturated transformers can be observed by comparing distortion results where the voltage present at the transformer is assumed to be undistorted for purposes of harmonic current injection calculation ("single-pass results") and distortion determined by the iterative algorithms.

Simple Circuits

The relative total harmonic voltage distortion (THD), as a function of GIC, is compared in Figure 4-2 for single-pass and converged iterated results. In this case, the system was modeled as a simple inductive source with a fundamental-frequency short-circuit capacity three times the transformer rating. At all GIC levels, the distortion calculated in single-pass analysis (first iteration) are significantly greater than the distortion found after the interaction between the system and the saturated transformer are fully accounted for in the final converged results.

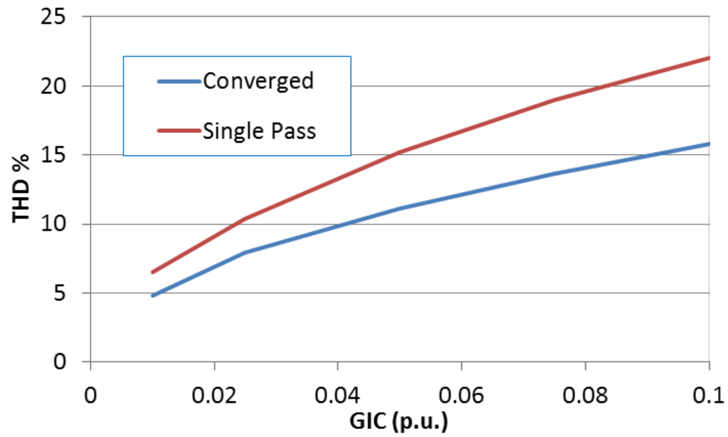

Figure 4-2
Comparison of total harmonic voltage distortion vs. GIC for a simple inductive source.

A different comparison is shown in Figure 4-3 for a more realistic and complex system representation. In this case, the system impedance equivalent is a series/parallel resonant network having a parallel resonance at 235 Hz (slightly below 4^{th} harmonic) and a series resonance at 340 Hz, as shown in the plot of impedance versus frequency in Figure 4-4. With this source impedance, the error in single-pass analysis is small at low values of GIC, but increase rapidly as the GIC level increases.

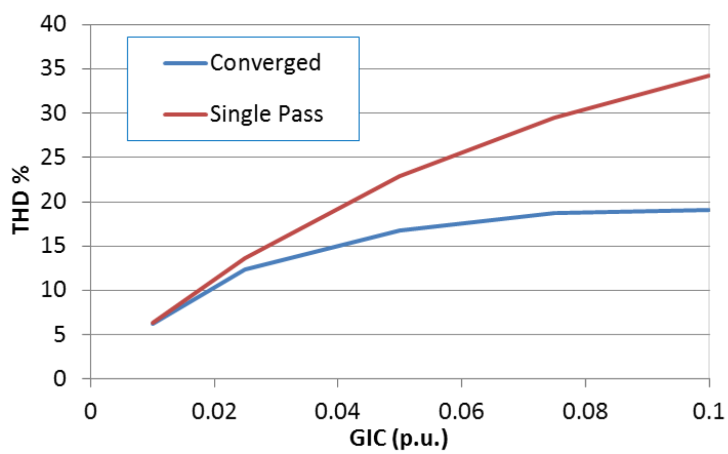

Figure 4-3
Comparison of total harmonic voltage distortion vs. GIC for a series/parallel resonant source network.

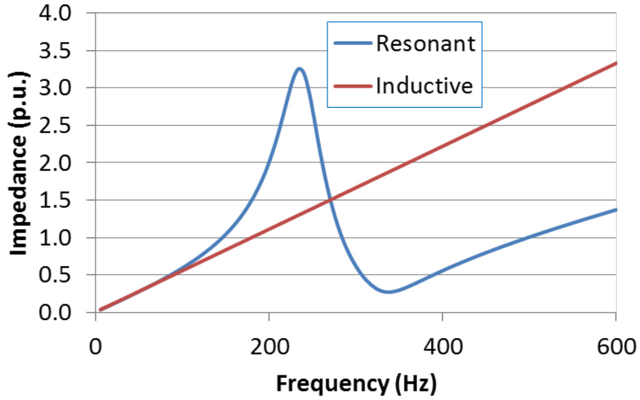

Figure 4-4
Impedance vs. frequency for the source representations used for Figure 4-2 (inductive) and Figure 4-3 (resonant).

Case Study Comparison

A more practical demonstration of closed-loop interaction between GIC-saturated transformers and system harmonic impedances, as well as interaction between different transformers, is demonstrated using the simple arbitrary system model shown in Figure 4-5. Conditions shown in Figure 4-5 are without GIC. A hypothetical GMD condition is assumed where an electric field magnitude of 10 V/mi is oriented along the length of the 200 mile transmission lines. As a result, a GIC flow of 449 A/phase results. The two transformers in this model absorb a total of 967 MVAR fundamental reactive power, resulting in the fundamental-frequency loadflow conditions shown in Figure 4-6. The EHV transmission line shunt reactors are assumed to be switchable, and these are switched out in the with-GIC loadflow solution. The least bus voltage is greater than 0.95 p.u., so this would not appear to be a severe scenario from a fundamental-frequency loadflow standpoint.

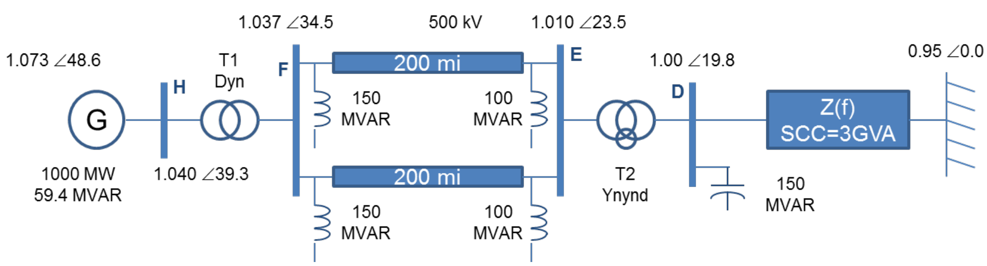

Figure 4-5
Case study system model and initial loadflow conditions without GIC.

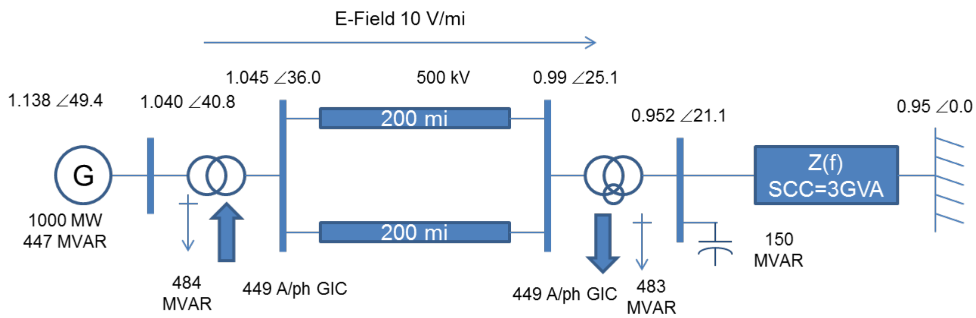

Figure 4-6
Case study model GIC and fundamental-frequency (loadflow) conditions with 10 V/mi E-field applied.

Harmonic distortion results for the case study model are compared in Figure 4-1 for single-pass analysis and a converged iterative solution. Harmonic distortion as determined by the simple single-pass analysis is very severe throughout the system. Capacitor rms current is very high, greater than typical capacitor fuse melting currents. The harmonic currents flowing into the generator cause a heating effect equivalent to 0.4 p.u. negative-sequence fundamental-frequency current, far greater than allowable by ANSI C50.13. Crest voltages are also high, due to the superposition of the harmonic voltage components on the depressed fundamental-frequency voltage, which could potentially result in surge arrester thermal instability and failure. These rather dire results are substantially less severe when distortions are calculated by a converged iterative solution. Further comparisons of the harmonic spectra of the capacitor and generator currents are shown in Figure 4-7 and Figure 4-8.

Table 4-1
Case Study Harmonic Results

Parameter	Single-Pass Analysis	Converged Solution
Bus D Voltage THD	37%	27%
Bus E Voltage THD	35%	25%
Bus F Voltage THD	24%	16%
Bus H Voltage THD	16%	10%
Bus H Crest Voltage (p.u.)	1.28 p.u.	1.18 p.u.
Generator Rotor Heating Current (equivalent to negative-sequence current, on generator base)	0.4 p.u.	0.25 p.u.
Capacitor Bank RMS Current (% of capacitor bank base)	158%	140%
Capacitor Bank Dielectric Heating (%kVA on capacitor bank base)	111%	106%

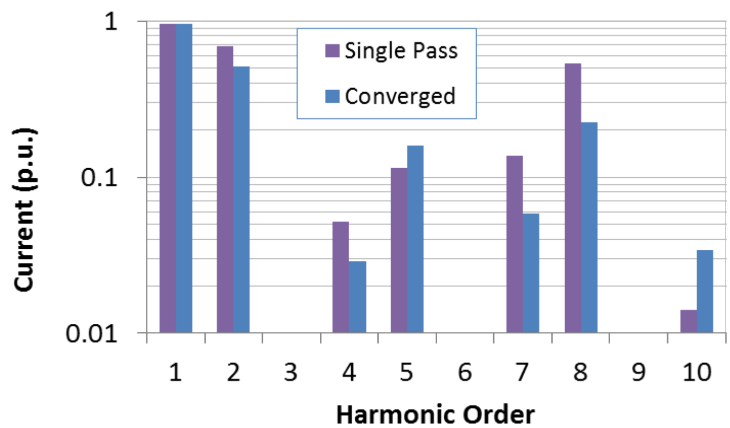

Figure 4-7
Capacitor bank harmonic current spectra, in p.u. of capacitor bank rating.

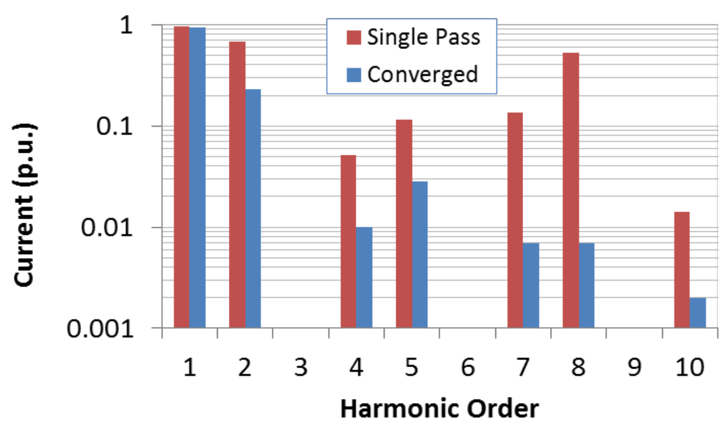

Figure 4-8
Generator harmonic current spectra, in p.u. of generator rating.

In addition to the comparison of first-pass versus final iterated results, this hypothetical case study also reveals interesting results about interactions between transformers at different locations. Figure 4-9 shows a phasor diagram for the second harmonic voltage component at Bus H. (The second harmonic is the dominant distortion component at this bus.) The diagram separately shows voltage components due to second harmonic currents injected by Transformers T1 and T2. It is interesting to note that the component due to T2 is the larger, despite the fact that this transformer is located 200 miles away from this bus, and T1 is connected directly to this bus. The two voltage contributions are substantially offsetting, with the resultant second harmonic voltage distortion of considerably less magnitude than either of the individual contributions. A comparison of similar phasor diagrams for first-pass analysis with the converged results reveals that the change in the resultant is primarily due to a change in the relative phase angles of the two voltage contribution components, more so than the change in component magnitude.

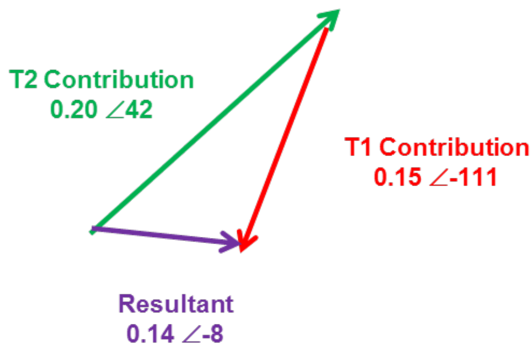

Figure 4-9
Bus H second harmonic voltage contributions from transformer T1 and T2 current injections.

5
ANALYSIS ALTERNATIVES AND REQUIREMENTS

Analysis of harmonic distortion caused by GMD can be performed using either frequency-domain (harmonic phasor) or time-domain forms of analysis. As described in the previous section, simple frequency domain analysis, for which the transformer harmonic current injections are based on the assumption of an undistorted fundamental voltage, is inaccurate and generally pessimistic. Such a “single pass” approach is, at best, is possibly sufficient for initial screening only. An accurate analysis requires proper consideration of the closed-loop interactions between the harmonic current injections by the saturated transformers and the voltage distortion that these injections cause. Thus, either an iterated frequency-domain analysis, or time domain simulation are the only alternatives for a comprehensive analysis of GMD-related harmonic distortion.

Common-Core Analysis Requirements

Whether time-domain or frequency-domain analyses of GMD-related harmonic performance are performed, there are certain core requirements that are applicable to either approach. These are:

1. Fundamental-frequency loadflow boundary conditions need to be maintained. This includes generator constant power and fundamental voltage (P-V bus) constraints, transformer tap changer adjustments, and constant real and reactive power loads, and automatic switching of reactive compensation. The fundamental frequency conditions are important because they establish the relative phase angles of the various harmonic current injections.
2. Modeling GIC flow to determine the magnitude and polarity of net GIC in each transformer is required.
3. Accurate modeling of the transformers subjected to GIC flow with transformer saturation settled out to the offset equilibrium condition (assuming that a steady-state GIC condition is to be modeled) is essential. Modeling of single-phase transformers is reasonably simple, and is described in this report. Modeling of three-phase transformers is more complex, and is beyond the scope of this report.
4. Accurate modeling of the reactances and resistances of the system at discrete harmonic frequencies, over the range of frequencies to be studied. Because the harmonic currents injected by GIC-saturated transformers generally decline with increasing harmonic order, it is generally sufficient to limit studies to the tenth harmonic and below. Accurate modeling requires attention to:
    a. Frequency-dependent branch impedance characteristics, including damping (resistance)
    b. Models of loads that exhibit realistic characteristics at harmonic frequencies
    c. Extent of the system model; a large system model is generally necessary
    d. Representation of both line and ground modes of harmonic propagation
5. A useful GIC analysis tool should allow a large number of system configurations to be evaluated with reasonable and practical applied effort.

Proper modeling of harmonic impedances presents several challenges. First of all, the impedances of each network branch must reflect appropriate frequency-dependent characteristics, including the resistive (damping) characteristics. Simple impedance representations, adequate for fundamental frequency, are often inadequate. For example, the X/R ratio of an actual power transformer tends to reach its peak below the third harmonic and decreases above this frequency. Transformer impedance is often represented in transient simulations, however, by a series resistance and inductance. The X/R of such a model rises indefinitely with frequency and is thus an inaccurate representation of transformer damping.

Another substantial modeling challenge is representation of reasonable characteristics for loads. At the low-order harmonic frequencies of importance to GMD events, loads are a substantial contributor of system damping. Loads, however, are not properly modeled by resistances and inductances simply based on their fundamental-frequency real and reactive power. Loads, particularly in North America, have a large motor component. At harmonic frequencies, these loads present far less damping than would be created by representing their fundamental power demand by a resistance.

To provide accurate driving point and transfer impedances for the low-order harmonics dominant in GMD-related distortion, the extent of the system model may need to be large. Typically, the model needs to extend for several hundreds of miles from the location of specific interest, or complex frequency-dependent source equivalent networks need to be derived, in order to adequately represent system impedance in this frequency range. System model extent requirements are also driven by the fact that transformer saturation at remote locations can contribute to the transformer saturation at a given bus.

GIC-saturated transformers inject harmonic currents in the line modes (positive and negative sequences) as well as the ground mode (zero sequence). In the case of single-phase transformer types, the zero sequence harmonics are orders equal to integer multiples of three (triplens). All other harmonics are line mode. Three-phase transformers, however, are asymmetric and any injected harmonic current may appear in a line mode or ground mode, or both.

System topology and branch impedances are different for the line and ground modes of harmonic propagation. For example, the frequency dependent characteristics of transmission lines are much more profound in the ground mode than the line modes, with both inductance and resistance varying with frequency. Delta transformer windings provide low inductance shunts for ground mode harmonics, and provide ground-mode isolation of parts of the grid (e.g., generators are isolated by their delta-wye step-up transformers). Typical transmission system harmonic analysis considers only the line mode harmonic propagation because the distorting devices or loads (e.g., industrial loads, SVCs, HVDC systems, etc.) are decoupled from the zero sequence of the transmission system by wye-delta transformers. As a result, many harmonic analysis tools are not well configured for ground mode analysis.

Harmonic impedances of the grid, including both driving point and transfer impedances, can be highly sensitive to the system configuration. In particular, status of individual capacitor banks and lines, and to a lesser extent, generators, can have a substantial effect on harmonic impedances. For this reason, harmonic analysis of a single, or small number of system configuration scenarios is generally inadequate to gain an understanding of harmonic related vulnerabilities of a system during severe GMD. It is generally necessary to perform a large number of combinations of system component status to perform a comprehensive study. For example, when harmonic performance specifications for HVDC and SVC are created, it is common to perform harmonic impedance studies where hundreds or even many thousands of configurations are analyzed to determine the range of harmonic impedance values. Thus, an approach facilitating efficient analysis of a large number of configurations, within reasonable time and resource constraints, is highly desirable.

Time Domain Analysis

GMD harmonic performance can be performed by time domain simulation using programs such as EMTP-RV, ATP, PSCAD, etc.

Pros

Time domain analysis has the following advantages:

1. Time domain analysis is conceptually simpler and less complicated than an iterative frequency domain analysis.
2. The proper phasing of harmonic current injections is inherent.
3. Closed-loop interaction between voltage distortion and transformer exciting current is also inherently incorporated.
4. Simulation programs that perform the analysis, at least where only single-phase transformers are involved, are readily available. (Gaps in three phase transformer models exist, but this deficiency applies equally to time and frequency-domain modeling.)
5. Transient simulation tools readily represent both line and ground mode propagation.

Cons

While the time-domain approach has strong advantages in its simplicity and availability, it suffers from some substantial disadvantages, including:

1. Time-domain simulation of GIC flow in a power system requires long simulation times in order for the offset saturation to settle out to the steady-state equilibrium. This is particularly true if transformers have low-resistance delta windings. It may take up to many tens of seconds of simulation time to reach the steady state, and time steps as short as twenty microseconds may be needed for proper operation and accuracy of the simulation program when modeling saturated transformers. The resulting one million time steps with a model with potentially large extent can require substantial computational resources and may make it impractical to consider a large number of system configurations and other scenarios.

   The long settling time is illustrated by the results shown in Figure 5-1, where a quasi-dc voltage source in series with a transmission line and terminated by a large grounded-wye delta generator step-up transformer. When the dc voltage source is turned on, the initial flow of current is impeded by the inductance of the transmission lines and the leakage impedance from the transformer grounded-wye windings to the delta winding. The direct current flow through the transmission lines reaches its steady-state value quickly (typically in less than a second), but in the transformer, the abrupt change of flow of dc into the grounded-wye winding induces an offsetting flow circulating in the delta winding. As a result, the transformer saturation does not begin immediately even though the GIC is flowing through the transformer. The circulating flow of quasi-dc in the delta times the delta winding’s relatively low dc resistance results in a small dc voltage. Because flux is the time integral of voltage, the flux offset increases slowly. Eventually, the transformer flux is sufficiently biased such that offset saturation begins as the flux peaks exceed the transformer saturation level. The circulating quasi-dc current in the delta winding decays and the rate of flux offset increase slows. Finally, the delta current decays to zero and the final equilibrium is reached.

2. Assembling large time-domain models can be unwieldy.
3. Use of the available time-domain transient simulation software requires rather specialized expertise.
4. Frequency-dependent representation of components such as transformers is not straightforward. While the expert user can create their own models, such as by using series/parallel resistance and inductance networks to represent transformer leakage impedance frequency-dependent damping, the typical user resorts to overly simplistic models which are inadequate.
5. Modeling loadflow constraints is difficult or impractical with some of the time-domain transient simulation software. The user typically needs to construct an interface with a separate loadflow program in order to import source parameters.
6. Load models present particular difficulties in transient simulation tools. This is primarily due to the profound difference in characteristics of induction motors at fundamental and at harmonic frequencies. While discrete induction motor models exist in these programs, it is impractical to create such models at every load bus in a large system model. Simplistic modeling of loads using passive resistances and inductances usually create unrealistic, and optimistic, levels of harmonic impedance damping.

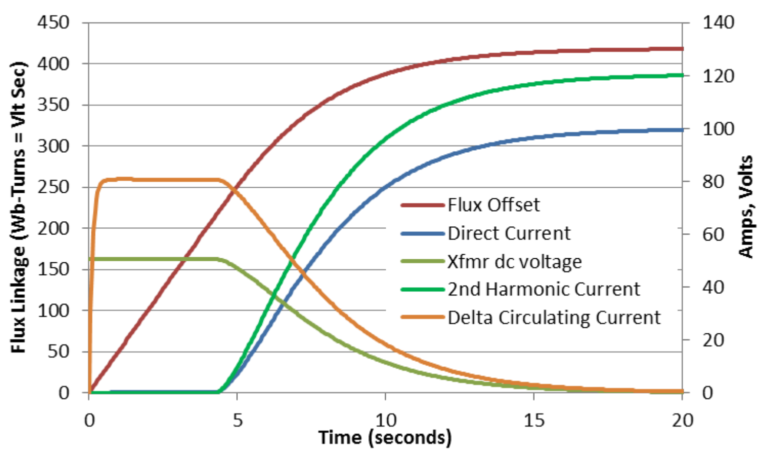

Figure 5-1
Dynamic response of a typical 400 MVA, 500 kV GSU transformer in a time-domain simulation where the induced quasi-dc voltage results in a steady-state 100 A/phase GIC.

Iterative Frequency-Domain Analysis

Frequency domain analysis of harmonic distortion during GMD has been extensively discussed in this report.

Pros

Frequency domain analysis has the following advantages:

1. Settling time is not a consideration; the program iterates to the final steady-state condition.
2. Relatively small incremental computational effort is needed to evaluate system configuration changes.
3. Frequency-dependent representation of system component impedances is easily implemented because the model does not need to represent multiple frequencies simultaneously. For example, the resistance can be programmed to vary as a defined function of frequency.
4. Realistic load modeling can be easily implemented for similar reasons.
5. The analysis can be integrated with loadflow analysis, drawing fundamental frequency voltage and current data, and the system database which can be used as the basis for conversion to a harmonic model.
6. The approach is compatible with large system models.
7. The software tools can be configured for use without a high level of specialized expertise required.

Cons

There are substantial disadvantages to the frequency-domain analysis approach, including:

1. Proper representation of the closed-loop interaction between the transformers and the system harmonic impedances, as well as one transformer with another, requires iterative analysis. There are no known commercially available software tools to perform this analysis.
2. The approach is somewhat complex, and proper attention to phase relationships, etc. is required in tool development.
3. In cases with very severe distortion, iterations may fail to converge.
4. Iterative frequency-domain analysis actually requires conversion back into the time domain at the local level for each transformer at each iteration, and then conversion back again to the frequency domain for system-wide analysis.

6
REMAINING RESEARCH NEEDS

This report describes an initial exploratory investigation of GMD-related harmonic distortion, revealing the significance of this GMD impact. The industry, however, needs both new tools and additional guidance in order to include harmonic issues in GMD impact assessments. Additional research and development is recommended to address the following gaps in capabilities and information:

1. This report has shown that simply calculating transformer harmonic current injections assuming undistorted voltage, and injecting these currents into a harmonic analysis, will yield seriously pessimistic results. While time-domain electromagnetic simulation tools such as EMTP-RV, ATP, and PSCAD are readily available and can be used to perform evaluation of harmonics during GMD, the time-domain approach is unwieldy and arguably impractical for performing analysis of a large number of scenarios. The report has documented an algorithm for performing an iterative frequency-domain analysis that correctly incorporates the complex closed-loop interactions between GIC-saturated transformers and the voltage distortion that they create. However, there is no tool available to the industry that can presently use this algorithm. Therefore, a recommended R&D activity is to develop such a frequency-domain analysis tool. Such a tool would be most useful to the industry if it is included within, or directly interconnects with the load flow programs used by the utility planning community.
2. Although a hypothetical case study described in this report shows harmonic impacts having far greater security significance than fundamental-frequency voltage issues, it is not known if this conclusion is specific to characteristics of this arbitrary model, or if this is a conclusion of more general validity. Performance of detailed harmonic analysis for several real systems, with results documented for the education of the industry, would go far to address this gap in present knowledge.
3. Modeling of three-phase transformers was not addressed in this report, but is very important to evaluation of GMD-related harmonic issues. There is a gap in the availability of models for these transformers that are sufficiently accurate and useable by the industry. In addition to models, there are large gaps in the available information detailing the magnetic designs of these transformers. Research to develop simple and useable models as well as guidance for modeling would be of great use to the industry.
4. With development of suitable three-phase transformer models and accumulation of sufficient transformer design data, research to characterize the harmonic current injection characteristics of these transformers would be a valuable guide to the industry. This research would be an extension of the characterization provided in this report for single-phase transformers.
5. The capability of some types of equipment, particularly capacitors and generators, to withstand high levels of harmonic distortion is documented in the standards. For many other types of equipment, this withstand capability is much less understood. Development of a guide to GMD-related harmonic impact evaluation would be of tremendous value to the industry. A common misconception is that the only system harmonic vulnerabilities are

related to protection system misoperation. A harmonic evaluation guide would place the various vulnerabilities in perspective and provide information needed for comprehensive GMD assessments.

7
REFERENCES

1. R. Pirjola, "On Currents Induced in Power Transmission Systems During Geomagnetic Variations", IEEE Transactions on Power Apparatus and Systems, Vol. PAS-104, No. 10, October, 1985, pp. 2825-2831.
2. J. Kappenman, "A Perfect Storm of Planetary Proportions", IEEE Spectrum, Vol. 49, Issue 2, 2012.
3. R. Girgis, K. Vedante, "Effects of GIC on Power Transformers and Power Systems", IEEE Power Engineering Society 2012 Transmission and Distribution Conference and Exposition
4. "Effects of Geomagnetic Disturbances on the Bulk Power System", 2012 Special Reliability Assessment Interim Report, North American Electric Reliability Corporation (NERC), February, 2012.
5. NERC Disturbance Analysis Working Group, "March 13, 1989 Geomagnetic Disturbance". Retrieved from http://www.nerc.com/files/1989-Quebec-Disturbance.pdf.
6. *Electromagnetic Transient-Type Transformer Models for Geomagnetically-Induced Current (GIC) Studies*. EPRI, Palo Alto, CA: 2013. 3002000832.
7. R. Walling, A. Khan, "Characteristics of Transformer Exciting Current During Geomagnetic Disturbances", IEEE Transactions on Power Delivery, Vol. 6, No. 4, October, 1991, PP 1707-1714.

A
APPENDIX

DERIVATION OF GIC AS A FUNCTION OF α

Assume a sinusoidal voltage with peak magnitude V_p. The resulting flux linkage is:

$$\lambda(t) = V_p \int \sin(\omega t)dt = -\frac{V_p}{\omega}\cos(\omega t) + \lambda_0 \tag{A1}$$

Now consider that the flux offset λ_0 is such that the instantaneous flux reaches the saturation level λ_s at α radians after the peak of the voltage at $\pi/2$ radians.

$$\lambda_s = -\frac{V_p}{\omega}\cos\left(\pi/2 + \alpha\right) + \lambda_0 = \frac{V_p}{\omega}\sin(\alpha) + \lambda_0 \tag{A2}$$

Solving for the flux offset and substituting into Equation A1:

$$\lambda_0 = \lambda_s - \frac{V_p}{\omega}\sin(\alpha) \tag{A3}$$

$$\lambda(t) = -\frac{V_p}{\omega}\left(\cos(\omega t) + \sin(\alpha)\right) + \lambda_s \tag{A4}$$

The exciting current when the flux surpasses the saturation level at time $\pi/2+\alpha$ is:

$$i(t) = \frac{\lambda(t)}{L_{ac}} = -\frac{V_p}{\omega \cdot L_{ac}}\left(\cos(\omega t) + \sin(\alpha)\right) + \lambda_s - \lambda_s = -\frac{V_p}{X_{ac}}\left(\cos(\omega t) + \sin(\alpha)\right) \tag{A5}$$

The dc component of the exciting current, which by definition is the GIC flow, is:

$$i_0 = \frac{1}{2\pi}\int_0^{2\pi} i(t) \cdot d(\omega t) = -\frac{V_p}{2\pi \cdot X_{ac}}\int_{\pi/2+\alpha}^{3\pi/2-\alpha}\left(\cos(\omega t) + \sin(\alpha)\right)d(\omega t) \tag{A6}$$

$$i_0 = -\frac{1}{2\pi} \cdot \frac{V_p}{X_{ac}}\left[\sin(\omega t) + \omega t \cdot \sin(\alpha)\right]_{\omega t = \pi/2+\alpha}^{\omega t = 3\pi/2-\alpha} \tag{A7}$$

$$i_0 = \frac{1}{2\pi} \cdot \frac{V_p}{X_{ac}}\left[2 \cdot \cos(\alpha) - \pi \cdot \sin(\alpha) + 2\alpha \cdot \sin(\alpha)\right] \tag{A8}$$

DERIVATION OF FUNDAMENTAL CURRENT AS A FUNCTION OF α

The fundamental component of the exciting current in Equation (A5), in quadrature to the voltage, is:

$$i_1 = \frac{1}{\pi}\int_0^{2\pi} i(t)\cdot\cos(\omega t)\,d(\omega t) = -\frac{V_p}{\pi\cdot X_{ac}}\int_{\pi/2+\alpha}^{3\pi/2-\alpha}\left[\left(\cos(\omega t)+\sin(\alpha)\right)\cdot\cos(\omega t)\right]d(\omega t) \tag{A9}$$

$$i_1 = -\frac{V_p}{\pi\cdot X_{ac}}\left[\frac{\omega t}{2}+\frac{\sin(2\omega t)}{4}+\sin(\alpha)\cdot\sin(\omega t)\right]_{\omega t=\pi/2+\alpha}^{\omega t=3\pi/2-\alpha} \tag{A10}$$

$$i_1 = \frac{V_p}{\pi\cdot X_{ac}}\cdot\left[\alpha-\frac{\pi}{2}-\frac{\sin(2\alpha)}{2}+2\sin(\alpha)\cdot\cos(\alpha)\right] = \frac{V_p}{2\pi\cdot X_{ac}}\cdot\left[2\alpha-\pi+\sin(2\alpha)\right] \tag{A11}$$

DERIVATION OF HARMONIC CURRENT COMPONENTS AS A FUNCTION OF α

The *cos(nωt)* (quadrature) harmonic terms of the Fourier expansion, i_{qn}, are:

$$i_{qn} = \frac{1}{\pi}\int_0^{2\pi} i(t)\cdot\cos(n\omega t)\,d(\omega t) = -\frac{V_p}{\pi\cdot X_{ac}}\int_{\pi/2+\alpha}^{3\pi/2-\alpha}\left[\left(\cos(\omega t)+\sin(\alpha)\right)\cdot\cos(n\omega t)\right]d(\omega t) \tag{A12}$$

$$i_{qn} = -\frac{V_p}{\pi\cdot X_{ac}}\cdot\left[\int_{\pi/2+\alpha}^{3\pi/2-\alpha}\left(\cos(\omega t)\cdot\cos(n\omega t)\right)d(\omega t)+\int_{\pi/2+\alpha}^{3\pi/2-\alpha}\left(\sin(\alpha)\cdot\cos(n\omega t)\right)d(\omega t)\right] \tag{A13}$$

$$i_{qn} = -\frac{V_p}{\pi\cdot X_{ac}}\cdot\left[\frac{\sin\left((1-n)\cdot(\omega t)\right)}{2\cdot(1-n)}+\frac{\sin\left((1+n)\cdot(\omega t)\right)}{2\cdot(1+n)}\cdot\frac{\sin(\alpha)}{n}\cdot\sin(n\omega t)\right]_{\pi/2+\alpha}^{3\pi/2-\alpha} \tag{A14}$$

$$i_{qn} = -\frac{V_p}{\pi\cdot X_{ac}}\cdot\left[\begin{array}{l}\dfrac{\sin\left((1-n)\cdot\left(3\pi/2-\alpha\right)\right)-\sin\left((1-n)\cdot\left(\pi/2+\alpha\right)\right)}{2\cdot(1-n)}+\\ \dfrac{\sin\left((1+n)\cdot\left(3\pi/2-\alpha\right)\right)-\sin\left((1+n)\cdot\left(\pi/2+\alpha\right)\right)}{2\cdot(1+n)}+\\ \dfrac{\sin(\alpha)}{n}\cdot\left(\sin\left(n\cdot\left(3\pi/2-\alpha\right)\right)-\sin\left(n\cdot\left(\pi/2+\alpha\right)\right)\right)\end{array}\right] \tag{A15}$$

For convenience, the terms of Equation (A15) are separated in order to continue the derivation separately for each term:

$$i_{qn} = -\frac{V_p}{\pi \cdot X_{ac}} \cdot \left[\frac{E}{2\cdot(1-n)} + \frac{F}{2\cdot(1+n)} + G \right] \tag{A16}$$

where:

$$E = \sin\left((1-n)\cdot\left(3\pi/2 - \alpha\right)\right) - \sin\left((1-n)\cdot\left(\pi/2 + \alpha\right)\right) \tag{A17}$$

$$F = \sin\left((1+n)\cdot\left(3\pi/2 - \alpha\right)\right) - \sin\left((1+n)\cdot\left(\pi/2 + \alpha\right)\right) \tag{A18}$$

$$G = \frac{\sin(\alpha)}{n}\cdot\left(\sin\left(n\cdot\left(3\pi/2 - \alpha\right)\right) - \sin\left(n\cdot\left(\pi/2 + \alpha\right)\right)\right) \tag{A19}$$

Simplifying the term *E*:

$$E = -\sin\left(\left(3n\pi/2 - 3\pi/2 - (n-1)\cdot\alpha\right)\right) + \sin\left(\left(n\pi/2 - \pi/2 + (n-1)\cdot\alpha\right)\right) \tag{A20}$$

$$E = -\cos\left(\left(3n\pi/2 - (n-1)\cdot\alpha\right)\right) - \cos\left(\left(n\pi/2 + (n-1)\cdot\alpha\right)\right) \tag{A21}$$

$$E = -\cos\left(\left(-3n\pi/2 + (n-1)\cdot\alpha\right)\right) - \cos\left(\left(n\pi/2 + (n-1)\cdot\alpha\right)\right) \tag{A22}$$

Applying the identity $cos(x) = cos(x + 2n\pi)$ where n is an integer:

$$E = -2\cdot\cos\left(n\pi/2 + (n-1)\cdot\alpha\right) \tag{A23}$$

Using similar simplification steps:

$$F = -2\cdot\cos\left(n\pi/2 + (n+1)\cdot\alpha\right) \tag{A25}$$

$$G = -2\cdot\frac{\sin(\alpha)}{n}\cdot\sin\left(n\pi/2 + n\cdot\alpha\right) \tag{A25}$$

Therefore:

$$i_{qn} = \frac{V_p}{\pi \cdot X_{ac}} \cdot \begin{bmatrix} -\dfrac{\cos\left(n\pi/2 + (n-1)\cdot\alpha\right)}{n-1} \\ +\dfrac{\cos\left(n\pi/2 + (n+1)\cdot\alpha\right)}{n+1} + \\ +2\cdot\dfrac{\sin(\alpha)}{n}\cdot\sin\left(n\cdot\left(\pi/2+\alpha\right)\right) \end{bmatrix} \tag{A26}$$

The *sin(nωt)* (direct) harmonic terms of the Fourier expansion, i_{dn} are found using similar steps:

$$i_{dn} = \frac{1}{\pi}\int_0^{2\pi} i(t)\cdot\sin(n\omega t)d(\omega t) = -\frac{V_p}{\pi \cdot X_{ac}}\int_{\pi/2+\alpha}^{3\pi/2-\alpha}\left[\left(\cos(\omega t)+\sin(\alpha)\right)\cdot\sin(n\omega t)\right]d(\omega t) \tag{A27}$$

$$i_{dn} = -\frac{V_p}{\pi \cdot X_{ac}}\cdot\left[\int_{\pi/2+\alpha}^{3\pi/2-\alpha}\left(\cos(\omega t)\cdot\sin(n\omega t)\right)d(\omega t) + \int_{\pi/2+\alpha}^{3\pi/2-\alpha}\left(\sin(\alpha)\cdot\sin(n\omega t)\right)d(\omega t)\right] \tag{A28}$$

$$i_{dn} = \frac{V_p}{\pi \cdot X_{ac}}\cdot\left[\frac{\cos\left((n-1)\cdot(\omega t)\right)}{2\cdot(n-1)} + \frac{\cos\left((n+1)\cdot(\omega t)\right)}{2\cdot(n+1)}\cdot\frac{\sin(\alpha)}{n}\cdot\cos(n\omega t)\right]_{\pi/2+\alpha}^{3\pi/2-\alpha} \tag{A29}$$

$$i_{dn} = \frac{V_p}{\pi \cdot X_{ac}}\cdot\begin{bmatrix} \dfrac{\cos\left((n-1)\cdot\left(3\pi/2-\alpha\right)\right)-\cos\left((n-1)\cdot\left(\pi/2+\alpha\right)\right)}{2\cdot(n-1)} + \\ \dfrac{\cos\left((n+1)\cdot\left(3\pi/2-\alpha\right)\right)-\cos\left((n+1)\cdot\left(\pi/2+\alpha\right)\right)}{2\cdot(n+1)} + \\ \dfrac{\sin(\alpha)}{n}\cdot\left(\cos\left(n\cdot\left(3\pi/2-\alpha\right)\right)-\cos\left(n\cdot\left(\pi/2+\alpha\right)\right)\right) \end{bmatrix} \tag{A30}$$

For convenience, the terms of Equation (A30) are separated in order to continue the derivation separately for each term:

$$i_{dn} = \frac{V_p}{\pi \cdot X_{ac}}\cdot\left[\frac{X}{2\cdot(n-1)} + \frac{Y}{2\cdot(n+1)} + Z\right] \tag{A31}$$

where:

$$X = \cos\left((n-1)\cdot\left(\tfrac{3\pi}{2}-\alpha\right)\right) - \cos\left((n-1)\cdot\left(\tfrac{\pi}{2}+\alpha\right)\right) \tag{A32}$$

$$Y = \cos\left((n+1)\cdot\left(\tfrac{3\pi}{2}-\alpha\right)\right) - \cos\left((n+1)\cdot\left(\tfrac{\pi}{2}+\alpha\right)\right) \tag{A33}$$

$$Z = \frac{\sin(\alpha)}{n}\cdot\left(\cos\left(n\cdot\left(\tfrac{3\pi}{2}-\alpha\right)\right) - \cos\left(n\cdot\left(\tfrac{\pi}{2}+\alpha\right)\right)\right) \tag{A34}$$

Simplifying the term X:

$$X = \cos\left(\left(\tfrac{3n\pi}{2} - \tfrac{3\pi}{2} - (n-1)\cdot\alpha\right)\right) - \cos\left(\left(\tfrac{n\pi}{2} - \tfrac{\pi}{2} + (n-1)\cdot\alpha\right)\right) \tag{A35}$$

$$X = \sin\left(\left(-\tfrac{3n\pi}{2} + (n-1)\cdot\alpha\right)\right) - \sin\left(\left(\tfrac{n\pi}{2} + (n-1)\cdot\alpha\right)\right) \tag{A36}$$

Applying the identity *sin(x) = sin(x+2nπ)* where *n* is an integer:

$$X = \sin\left(\left(\tfrac{n\pi}{2} + (n-1)\cdot\alpha\right)\right) - \sin\left(\left(\tfrac{n\pi}{2} + (n-1)\cdot\alpha\right)\right) = 0 \tag{A37}$$

Using similar simplification steps:

$$Y = Z = 0 \tag{A38}$$

Therefore,

$$i_{dn} = 0 \tag{A39}$$

Thus, for a voltage defined as $V_p \cdot \sin(\omega t)$, the harmonic components of exciting current are exclusively the cosine terms of the Fourier expansion:

$$i_n(t) = \frac{V_p}{\pi\cdot X_{ac}}\cdot\left[-\frac{\cos\left(\tfrac{n\pi}{2}+(n-1)\cdot\alpha\right)}{n-1} + \frac{\cos\left(\tfrac{n\pi}{2}+(n+1)\cdot\alpha\right)}{n+1} + 2\cdot\frac{\sin(\alpha)}{n}\cdot\sin\left(n\cdot\left(\tfrac{\pi}{2}+\alpha\right)\right)\right]\cdot\cos(n\omega t) \tag{A40}$$

3002002985

Electric Power Research Institute
3420 Hillview Avenue, Palo Alto, California 94304-1338 • PO Box 10412, Palo Alto, California 94303-0813 • USA
800.313.3774 • 650.855.2121 • askepri@epri.com • www.epri.com